

15th DOE NUCLEAR AIR CLEANING CONFERENCE

SESSION VIII

DAMAGE CONTROL

Tuesday, August 8, 1978
CHAIRMAN: W. L. Anderson

IN-DUCT COUNTERMEASURES FOR REDUCING FIRE-GENERATED-SMOKE-AEROSOL EXPOSURE TO HEPA FILTERS
N. J. Alvares, D. G. Beason, H. W. Ford

AIR CLEANING SYSTEM ISOLATION DURING TORNADO CONDITIONS
W. A. Pysh, T. A. Clements

EVALUATING NUCLEAR POWER PLANT VENTILATION SYSTEM ADEQUACY IN REDUCING AIRBORNE RADIOACTIVITY EXPOSURE
W. E. Jouris

AIR CLEANING SYSTEMS ANALYSIS AND HEPA FILTER RESPONSE TO SIMULATED TORNADO LOADINGS
W. S. Gregory, R. W. Andrae, K. H. Duerre, H. L. Horak, P. R. Smith, C. I. Ricketts, W. Gill

OPENING REMARKS OF SESSION CHAIRMAN:

This session will address several aspects of damage control of particulate filtration devices utilized in nuclear installations. Four papers are included on the agenda; however, these will address only two of the many threats for potential system damage. Two of the papers will describe the determination of pressure differential under tornado conditions and the response of the various filtration/protective components to these conditions. A third paper addresses potential countermeasures against fire conditions and fire generated aerosols, while the fourth will describe a total evaluation of system adequacy for reducing airborne exposure.

15th DOE NUCLEAR AIR CLEANING CONFERENCE

IN-DUCT COUNTERMEASURES FOR REDUCING FIRE-GENERATED-SMOKE-AEROSOL EXPOSURE TO HEPA FILTERS *

N. J. Alvares, D. G. Beason, H. W. Ford
Lawrence Livermore Laboratory
University of California
Livermore, California

Abstract

An experimental program was conducted to assess the endurance and lifetime of HEPA filters exposed to fire-generated aerosols, and to reduce the aerosol exposure by installing engineering countermeasures in the duct between the fire source and HEPA filters.

Large cribs of wood and other potential fuels of interest were "forcefully burned" in a partially ventilated enclosure. In a "forceful burn" the crib of fuel is continuously exposed to an energetic premixed methane flame during the entire experimental period. This tactic serves two purposes: (1) It optimizes the production of smoke rich in unburned pyrolyzates which provides severe exposure to the filters, and (2) It facilitates the ignition and enhances the combustion of cribs formed with synthetic polymers.

The fuel cribs vary in size but have similar weight (~ 200 kg). The crib elements were natural and synthetic polymers; i.e., polyvinyl chlorides, polymethyl methacrylate (fire retarded), polycarbonate, dense fiberboard, wood, or combinations thereof. These elements are approximately 16 cm^2 in cross sectional area by 90 and 120 cm in length. The elements are either closely packed where the spacing dimensions are identical to the element cross section, or relatively loosely packed where the elements are supported by a metal framework. Some of these materials required a metal framework with a wire screen "floor" at alternate layers to prevent sagging. Wood cribs supported by the same type of framework burned at a faster rate, indicating a somewhat greater lateral crib porosity.

The experiments were conducted in an enclosure specifically designed and instrumented for fire tests. The test cell has a volume of 100 m^3 and includes instrumentation to measure the internal temperature distribution, pressure, thermal radiation field, flow fields, gas concentration, particulate size distribution and mass, fuel weight loss, inlet and exit air velocities, and smoke optical density.

The countermeasure techniques include the use of passively operated sprinkler systems in the fire test cell, of fine and dense water scrubbing sprays, and of rolling prefiltration systems in the exit duct of the fire test cell. Of the countermeasures surveyed, the rolling prefilter system showed the most promise, since it extended HEPA filter lifetimes by factors of two or more.

This paper will concentrate on the effect of control variables; i.e., enclosure air supply, fuel composition and crib porosity, and on the combustion response; i.e., crib burning rate, enclosure temperature rise, oxygen consumption, and CO , CO_2 and total hydrocarbon production. A discussion of the attempts to rationalize smoke aerosol properties, i.e., aerosol mass-and-size distribution on filter plugging phenomena will be included along with results from the effect of countermeasure application on HEPA filter lifetimes.

*Work performed under the auspices of the U.S. Department of Energy by the Lawrence Livermore Laboratory under contract No. W-7405-Eng-48.

15th DOE NUCLEAR AIR CLEANING CONFERENCE

I. Introduction

An unwanted fire in a space containing radioactive materials can compromise containment measures more dramatically than any threat other than explosion as fire can reduce solids and liquids to aerodynamic aerosols and provide the convective flow to distribute them. The methods by which fire defeats standard containment devices and practices include:

- Overpressurizing the space by generating more gas than can flow through the ventilation.
- Overpressurizing the space by plugging the HEPA filters in exhaust ducts with smoke aerosol.
- Breaching the filter by temperature degradation of the filter media.
- Penetrating the filter with evaporated volatile pyrolysis fractions.

We have attempted to identify through testing some practical and cost-effective countermeasures that will, for a reasonable period, protect HEPA filters from the products of such fires. While a normal HEPA filter lasts from 6 to 24 mo depending on exposure conditions, the duration of exposure prior to HEPA plugging or high-temperature breaching during a severe and smoky fire may be reduced to 5 min. Exposure duration is controlled by the type and geometry of the fuel and by the ventilation patterns of the enclosure. Thus, the device or procedure ultimately used as a countermeasure to protect HEPA systems from potentially high smoke and heat exposure must be capable of increasing the smoke exposure filtration so it lasts through the fire brigade attack and until the source fire is controlled.

The primary purpose of our tests then is to make smoke; this we do in the test cell shown schematically in Fig. 1. We described this test cell and its capabilities in detail in the 14th Conference⁽¹⁾ along with details of some preliminary

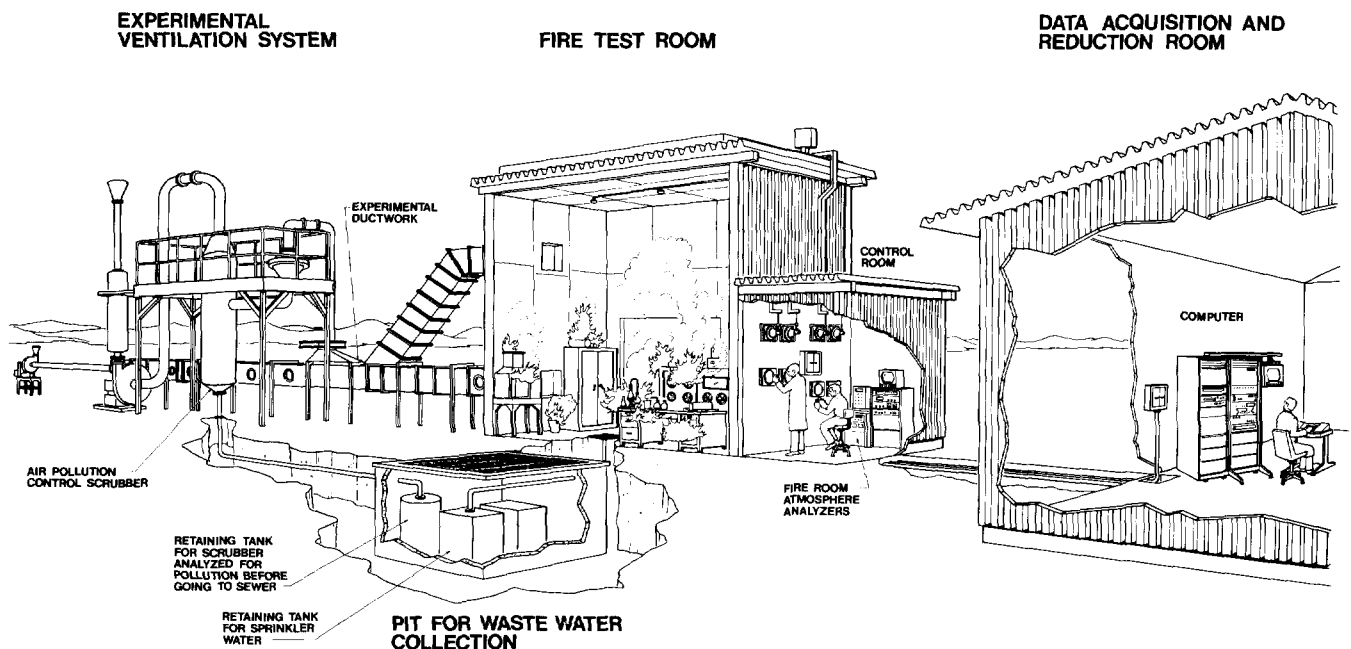
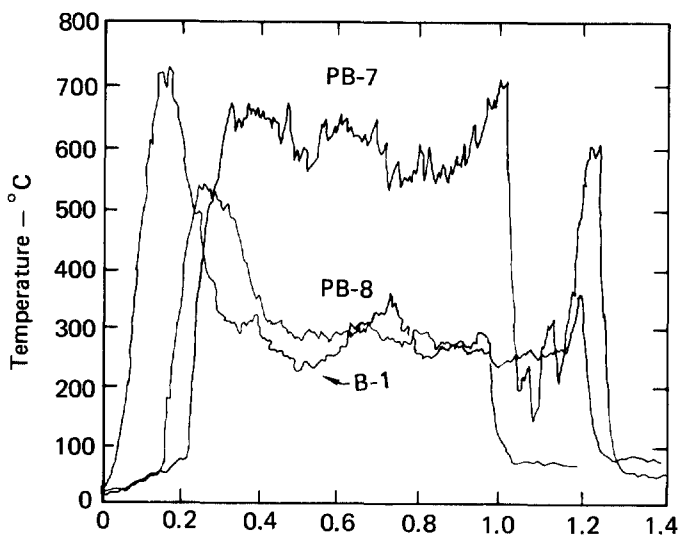


Fig. 1. Full-scale fire test facility.

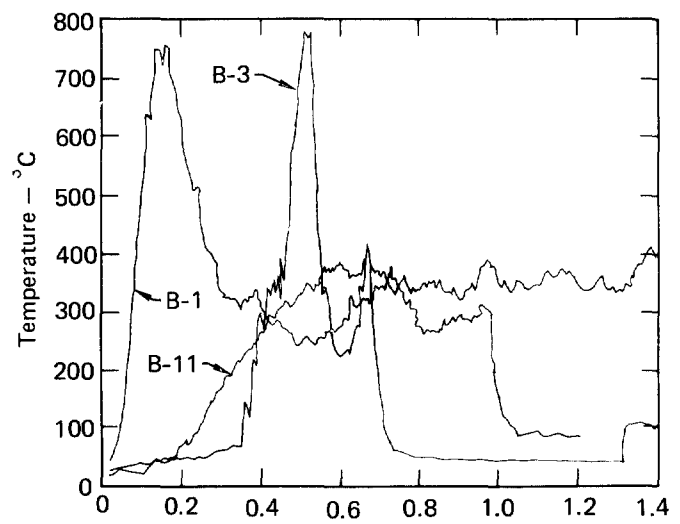
15th DOE NUCLEAR AIR CLEANING CONFERENCE

The effects of crib spacing and ventilation rate on crib burning are shown in Fig. 3. The differences in time to peak burning for PB-8 and B-1 illustrate the effect of crib porosity. However, they exhibit a similar trend due to the effects of ventilation control of the combustion processes; that is, temperature reduction after a high intensity phase was indicative of oxygen starvation in tests PB-8 and B-1. In test PB-7, however, the ventilation rate was sufficient to allow active combustion over the entire test period.

Figure 4 indicates how the characters of different burning polymers compared to that of a fir wood crib. The B-3 curve illustrates the behavior of a fire-retarded PMMA* by its temperature response; although it takes a relatively long time to ignite, once ignited it burns with fierce intensity. The combustion response of polycarbonate is shown by the B-11 labeled curve. Once ignited, polycarbonate burns steadily with moderate heat and smoke release.



Time - ks
 B-1 ⇒ open crib, 250 l/S
 PB-8 ⇒ closed crib, 250 l/S
 PB-7 ⇒ closed crib, 500 l/S



Time - ks
 1 ⇒ Firwood crib, 250 l/S
 B-3 ⇒ PMMA - FR crib, 250 l/S
 B-11 ⇒ Polycarbonate, 259 l/S

Fig. 3. Effects of crib spacing and ventilation rate on crib burning.

Fig. 4. Comparison of the characters of burning polymers to that of a fir wood crib.

Figure 5 illustrates the selected fir and airflow parameters we surveyed during each test. Burn 29 was a supported wood crib (i.e., the standard fuel array used for correlation tests). The displayed data are: plume temperature ($T^{\circ}\text{C}$), oxygen concentration [O_2], burning rate or fuel consumption (\dot{m}), airflow through the ventilation duct (\dot{V}), and pressure drop across the HEPA filter (ΔP_{HEPA}). When airflow through the HEPA filter reached half the initial flow rate, indicated by the cross on the airflow curve, we considered the filter plugged and terminated the test. We conducted comparative analyses with data taken at the temperature peak and again just prior to significant flow reduction. (In Fig. 5, this would be approximately 400 s). Along with the indicated data, we measured total aerosol concentration and rough aerosol size distribution at the exit to the test cell and just upstream of the HEPA filter. Moreover, we used cryogenic techniques to trap grab samples of aerosol and combustion gas both up and downstream of the filter for chemical analysis.

* Polymethylmethacrylate

15th DOE NUCLEAR AIR CLEANING CONFERENCE

tests in which we installed laboratory furnishings and appliances in the test cell as fuel items. We indicated a major problem with using such items in a quasi-normal array was the nonuniformity of the flame spread and, consequently, of the smoke production. What we needed was a reproducible but severe source of smoke so we could appraise the effects of various countermeasures to increase the smoke exposure lifetimes of HEPA filters.

Our solution was to employ cribs (cross piles of fuel) a fuel array traditionally accepted in fire research. We selected our fuel elements from materials abundant in laboratories where radioactive materials are used or stored. We tested several crib arrangements and fuel element distributions, finally deciding on a series of configurations particular to various fuels that would provide a moderate fuel load (1 to 2 lb/ft²) for the test cell. Figure 2 shows three crib arrays: the top plate shows a natural crib of wood with element dimensions of 1.5 in. on a side and 3.5 ft in length. This crib has a relatively low porosity (i.e., very close element spacing), which reduces the burning rate of the fuel. The second plate shows a crib of wood whose alternate layers are supported on a metal framework. The framework supports plastic fuels that soften and flow during flame exposure, as shown in the third plate of Fig. 2. Since a significant proportion of our fuels are synthetic polymers, we have opted to contain all fuel elements in the same type of support grid. This geometry results in a somewhat higher porosity than the natural crib; hence, the burning characteristics are accelerated.



Plate 1

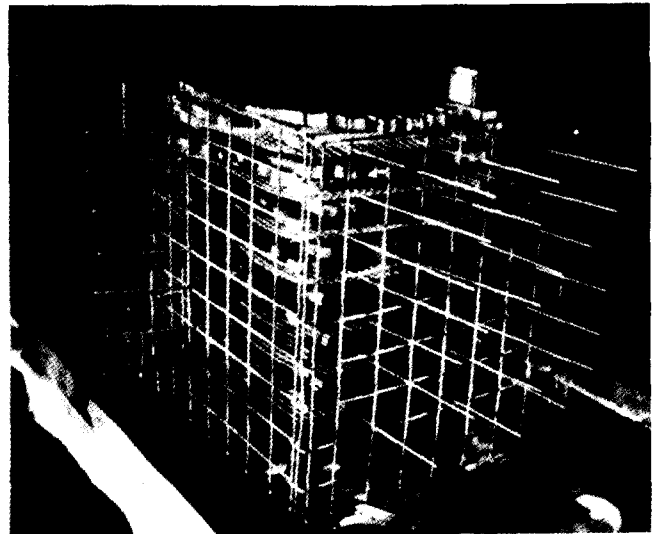


Plate 3

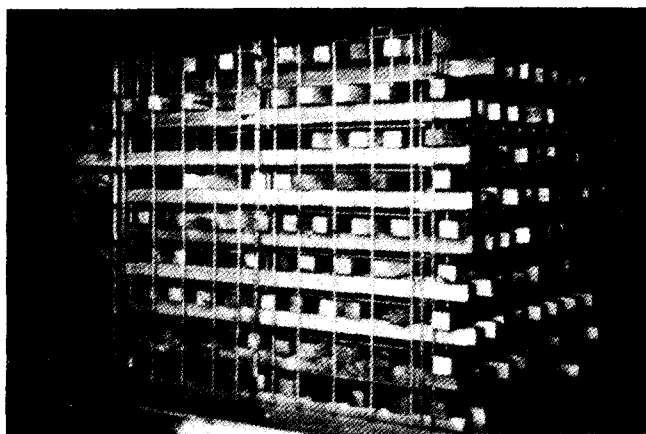


Plate 2

Fig. 2. Crib arrangements for fire tests.

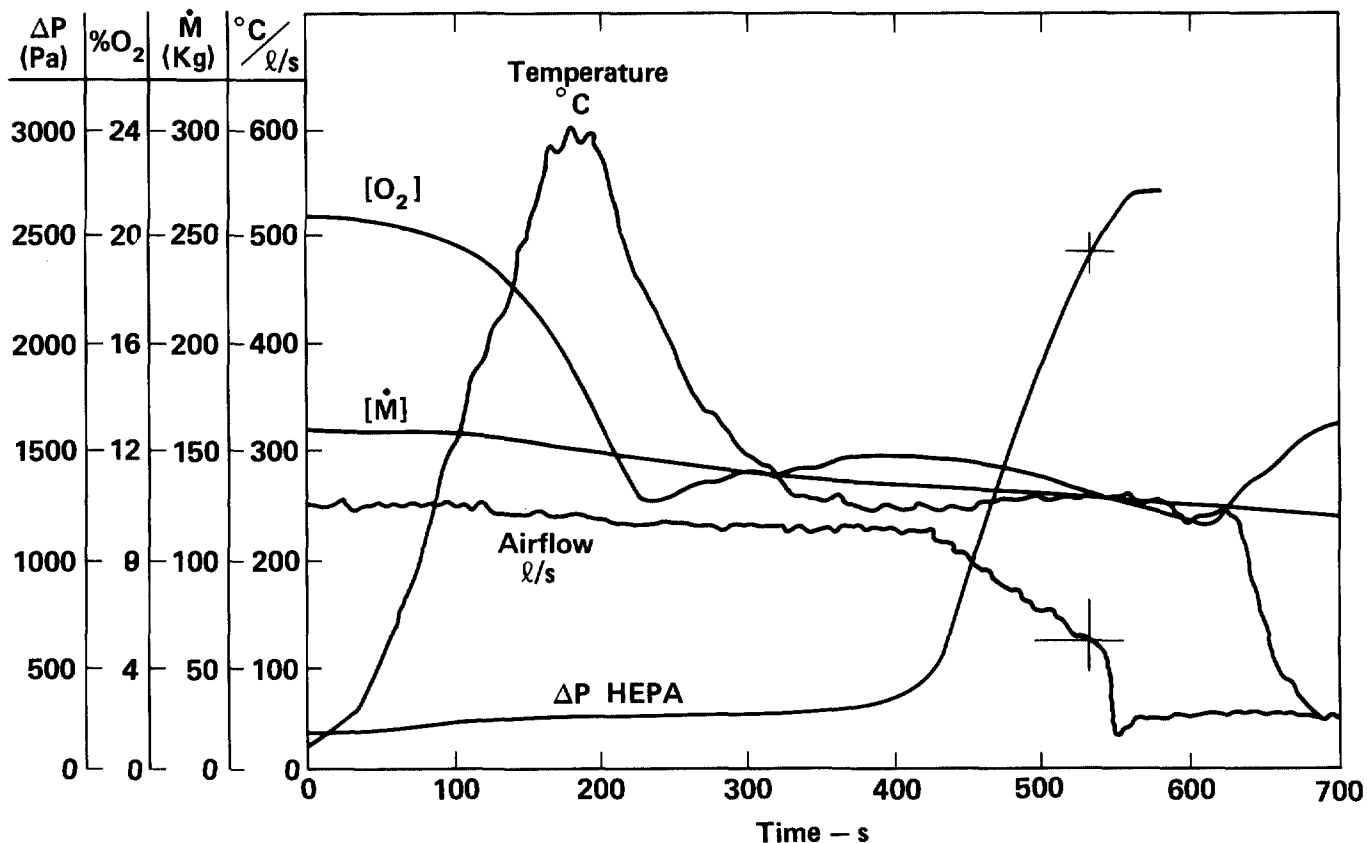


Fig. 5. Selected fire and airflow parameters.

II. Measurements

Because our ignition burner continues to burn throughout the exposure, our crib fires very likely produce more smoke aerosols than would a free-burning crib. For the same reason, the induction period to full burning intensity and, subsequently, to ventilation control is shorter. We are thus able to describe and control the dynamic aspects of our fire source with some degree of success; that is, given the material and a description of the crib parameters, we can approximately predict the combustion response. However, we have been totally unsuccessful in our attempts to characterize smoke aerosols. We can gain some idea of the magnitude of excess pyrolyzate* by comparing the measured weight loss, \dot{m} , to the fuel consumption potential as calculated by the oxygen consumption during a stoichiometric combination of fuel and oxygen to products⁽³⁾. Table 1 shows this comparison for some early tests and indicates an order-of-magnitude estimate of the unburned pyrolyzate, which, in almost all cases, is of the same magnitude or of greater magnitude than the burned fractions.

Our attempts to measure the size and mass distribution of smoke aerosols were fraught with complications, mainly because of the high aerosol concentration as indicated in Table 1. Moreover, the chemical and physical interactions in dense aerosols from any source made such measurements almost impossible. Kinetic processes such as agglomeration, evaporation, deposition, gradation, fallout electrostatics, chemical change, and adsorption caused the aerosol to change its character during both sampling and measurement procedures. Regardless of these complications, we took a continuous series of aerosol mass and mass distribution measurements using cascade impactors positioned near the exit to the test cell and at the upstream surface of the HEPA filter. Table 2 summarizes these measurements.

* Partially oxidized pyrolysis fractions that can occur during ventilation-limited combustion processes.

15th DOE NUCLEAR AIR CLEANING CONFERENCE

Table I. Gross estimates of excess pyrolyzate.

Test	Material	Measured fuel mass loss, \dot{m}_f (kg/s)	Calculated fuel consumption from oxygen depletion measurements, \dot{m}_o (kg/s)	Gross excess pyrolyzate, $\dot{m}_f - \dot{m}_o$ (g/s)
PB-7	Fir wood ^a	0.13	0.086	44
B-1	Fir wood	0.12	0.041	89
B-3	PMMA-FR ^b	0.028	0.003	25
B-11	Polycarbonate	0.037	0.019	18
B-15	Dense fiberboard	0.080	0.049	31
B-17	Polyvinyl chloride	0.020	0.008	12
B-18	Fiber-reinforced polyester	0.020	0.020	0
B-20	Composite ^c	0.020	0.016	4
B-21	Fir wood ^d	0.10	0.043	57
B-28	Fir wood ^e	0.1/0.06 ^g	0.038	42 ^h
B-36	Fir wood ^f	0.097/0.058 ^g	0.089	8
B-38	Composite	0.05	0.023	27

^a 500-ℓ/s air supply and low-porosity crib.

^b Polymethylmethacrylate – fire retarded.

^c Crib made with fir wood, PMMA-FR, polycarbonate, fiber-reinforced polyester, and polyvinyl chloride.

^d Low air intake and exhaust duct.

^e High air intake and exhaust duct.

^f 500-ℓ/s air supply.

^g Varies with time for high air intake and exhaust duct tests.

^h Based on average \dot{m}_f .

TABLE II. Cascade impactor data

Test	Material for crib	Impactor at exit of test cell			Impactor at HEPA station				
		Conc, kg/m^3	Gross mass distribution %			Conc, kg/m^3	Gross mass distribution %		
			$d > 3$	$d > 1$	$d < 1^a$		$d > 3$	$d > 1$	$d < 1^a$
PB-7	Tight fir wood					0.001	82	2	16
B-2	Loose fir wood					0.005	3	60	37
B-3	PMMA-FR					0.001	3	44	53
B-11	Polycarbonate					0.0007	14	58	28
B-15	Dense fiberboard	0.002	12	71	17	0.002	6	67	27
B-17	Polyvinyl chloride	0.002	10	69	21	0.002	10	63	27
B-18	Fiber-reinforced polyester	0.001	61	21	18	0.002	56	15	29
B-20	Composite	0.006	42	57	1	0.005	25	72	3
B-21	Loose fir wood	0.013	62	32	6	0.009	49	23	28
B-28	Loose fir wood	0.006	68	25	7	0.002	89	0	11

^a d = Aerosol diameter in microns.

TABLE IV. Fir wood crib ventilation and fuel moisture variables

Test	Date	Ventilation Inlet / Exhaust	\dot{m} , ^a kg/s	t_{peak} , ^b s	t_{plug} , ^c s	$\frac{t_{\text{peak}}}{t_{\text{plug}}}$, ^s	T_{av} , ^d °C	T_{db} , ^e °C
B-2	7/76	Low / High	0.12	160	330	2.07	224	100
B-13	4/77	Leak / High	0.07	210	610	2.9	183	105
B-21	7/77	Low / Low	0.10	140	570	4.0	215	90
B-28	11/77	High / High	0.1 0.05	190	540	2.85	172	110
B-30	2/78	High / High	0.077 0.047 0.038	190	No plug	---	160	120
B-32 (dry)	3/78	High / High	0.12 0.03	160	310	1.9	185	112

^a \dot{m} = burning rate.

^b t_{peak} = time to peak temperature above crib.

^c t_{plug} = time to HEPA plugging.

^d T_{av} = average highest test cell temperature.

^e T_{db} = dry bulb temperature at HEPA.

cellulosic fuels of high moisture content would burn at a much slower rate than the sensible removal of water from the cellulose would indicate⁽⁴⁾. To test this finding, we kiln dried enough wood for one crib load. The average moisture content of the dried elements was less than 6%. The results are shown in test B-32 where plugging occurred in 310 s. Obviously, control of the moisture content of porous fuels is very important to ensuring reproducibility in tests.

We have tried several countermeasures to keep the HEPA filter from plugging, including rolling prefiltration, increasing the HEPA surface, water scrubbing, stopping the fire with sprinklers, and controlling the materials. Table 5 summarizes our countermeasure experience and condenses the data given in Table 3 to specifically address the relative merits of different countermeasure techniques.

15th DOE NUCLEAR AIR CLEANING CONFERENCE

The weighing protocol for most measurements listed in Table 2 called for holding the filter papers at 60°C for 24 hr before and after measurement. Obviously, we lost all volatile fractions that vaporize at temperatures below 60°C. Even so, the total concentration of solid-phase aerosol appeared to range around 0.002 kg/m³ (2 g/m³). Note, that while we indicate size range, we view these data with reservation. Our total mass measurements of solid-phase aerosol are probably as reliable as anyones.

We knew that by drying the filter after aerosol sampling, we were losing some proportion of the actual in duct aerosol mass. We determined this by sealing the impactors after sampling and by weighing the filters as soon as possible after terminating the test. Then we dried the filters at 60°C and reweighed them. The difference in total mass between the initial and final weighing was a factor of 6 at both the test cell exit and the HEPA exposure surface. Subsequent measurements indicated mass distribution shifts from large ($d > 3\mu$) to small ($d < 1\mu$) particles - an expected trend.

III. HEPA Filter Performance

Table 3 summarizes HEPA filter performance for all tests conducted during this experimental series. Included in the table are fuel consumption (\dot{m}), oxygen depletion ($[O_2]$), time to filter plugging (t_{plug}), dry bulb temperature at the filter (T_{DB}), measured total aerosol mass at t_{plug} and calculated excess pyrolyzate. These data show the remarkable ability of HEPA filters to perform well even when exposed to very dense aerosol loads. The shortest time to plug, for an unprotected filter was 320 s, and the measured maximum aerosol mass was 7 gm/m³ (measured from a dry impactor filter array). Since the flow was 250 l/s, the imposed aerosol load was at least 1.75 gm/s and was quite likely much more.

An aspect that modified filter performance was the temperature level at the HEPA station. For dry bulb temperatures of 120°C or higher, the time to plug was significantly longer; in some cases at high temperatures, the filter did not plug. It appeared that some major plugging components of the smoke aerosols remained in gas phase at temperatures greater than 110°C and, consequently, were not adsorbed by the HEPA. This observation was supported by the fact that condensed vapors were observed leaving the exit stack when high-temperature conditions were maintained in the duct and by the chemical determination of hydrocarbon compounds from grab samples taken downstream of the filter.

Table 4 shows that fuel condition and ventilation variables can also affect the HEPA's plugging performance.* The major variable here was supposed to be the ventilation pattern in the test cell, which was equipped with a high and low exit port and two high and low air-inlet ports. [We always use two air inlets (low or high) and one exit port (low or high)]. The first column lists the test number, date, and inlet/exit configuration. The data show that \dot{m} did not vary drastically with the ventilation pattern except for test B-13, where we closed the inlet and found our test cell leaked almost as well as our inlet ducts. [We have subsequently sealed all leaks.]

We also noted that with the Hi/Hi ventilation configuration, the \dot{m} measurement appeared to have a variable character. Most baffling, however, was test B-30; here the filter did not plug. True, the T_{DB} reached 120°C, but we had plugged filters with this condition before. On checking our fuel, we found the wood elements had a 20% average moisture content. Our literature search indicated

* These data are from wood cribs only.

15th DOE NUCLEAR AIR CLEANING CONFERENCE

Table III. Review of test data and HEPA filter response for May 28, 1976 to July 15, 1978.

Test	Fuel	Geometry	Countermeasure	Ventilation rate (l/s)	Ventilation geometry Inlet/Outlet	Rate of measured fuel mass loss, mf (kg/s)	Oxygen depletion (%)	Dry bulb temperature at HEPA, T _{db} (°C)	Time to plug, t _p (kg)	Calculated excess pyrolyzate (g/s)	Measured aerosol mass (g/m ³)
PB-7	Fir wood	Nonporous crib	Free burn	500	Low/High	0.13	15.6	185	0.90	44	1.0
PB-8	Fir wood	Nonporous crib	Free burn	250	Low/High	0.09	14.5	90	0.70	50	12.0
PB-8.2	Fir wood	Nonporous crib	Free burn	250	Low/High	0.10	15.0	100	0.70	59	5.0
B-1	Fir wood	Supported crib	Free burn	250	Low/high	0.13	15.0	100	0.32	89	7.2
B-2	Fir wood	Supported crib	Free burn	250	Low/High	0.12	16.0	100	0.37	76	4.6
B-3	PMMA-FR	Supported crib	Free burn	250	Low/High	0.028	1.6	50	0.40	25	4.1
B-4	PMMA-FR	Supported crib	Free burn	500	Low/High	0.11	7.4	110	1.45	85	1.4
B-5	Diesel oil	3-ft pan	Free burn/scrubbers	250	Low/High	—	—	—	—	—	—
B-6	Fir wood	Supported crib	Scrubber	250	Low/High	0.10	16.0	59	0.37	56	2.2
B-7	Fir wood	Supported crib	Scrubber	250	Low/High	0.11	17.0	31	0.38	63	3.5
B-8	Fir wood	Supported crib	Scrubber	250	Low/High	0.10	17.2	60	0.32	53	1.5
B-9	Fir wood	Supported crib	Fusing sprinkler	250	Low/High	—	12.0	100	No plug	—	—
B-10	PMMA-FR	Supported crib	Fusing sprinkler	250	Low/High	—	2.0	58	0.40	—	—
B-11	Polycarbonate	Supported crib	Free burn	250	Low/High	0.037	12.0	80	No plug	18	—
B-12	Polycarbonate	Supported crib	Fusing sprinkler	250	Low/High	—	4.5	65	0.55	—	—
B-13	Fir wood	Supported crib	Inlet dampers closed	250	Low/High	0.07	16.0	105	0.61	26	—
B-14	Fir wood	Supported crib	Free burn	250	Low/High	0.12	17.5	120	0.67	72	—
B-15	Dense fiberboard	Supported crib	Free burn	250	Low/High	0.08	17.9	110	No plug	31	1.7
B-16	Dense fiberboard	Supported crib	Fusing sprinkler	250	Low/High	—	3.4	75	No plug	—	—
B-17	Polyvinyl chloride	Supported crib	Free burn	250	Low/High	0.02	3.6	60	0.59	12	2.1
B-18	Fiber-reinforced polyester	Supported crib	Free burn	250	Low/High	0.02	12.7	90	0.88	—	1.6
B-19	Fiber-reinforced polyester	Supported crib	Fusing sprinkler	250	Low/High	—	3.5	80	No plug	—	—
B-20	Composite	Supported crib	Free burn	250	Low/High	0.02	8.0	100	0.40	4	6.4
B-21	Fir wood	Supported crib	Free burn	250	Low/Low	0.10	15.8	90	0.57	57	—
B-22	Fir wood	Supported crib	Free burn	250	Low/Low	0.08	18.2	95	0.76	30	—
B-23	Composite	Supported crib	Rolling prefilter	250	Low/High	0.07	12.2	45	No plug	36	13.7
B-24	Composite	Supported crib	Rolling prefilter	250	Low/High	0.07	14.0	35	No plug	32	3.3
B-25	Composite	Supported crib	Rolling prefilter	250	Low/High	0.06	14.0	—	No plug	22	—
B-26	Fir wood	Supported crib	Rolling prefilter	250	Low/High	0.08	19.0	70	No plug	28	16.8
B-27	Fir wood	Supported crib	Prefilter circuit only	250	Low/High	0.09	17.8	80	0.72	41	—
B-28	Fir wood	Supported crib	Free burn	250	High/High	0.1-0.06	13.8	110	0.44	42	27.0
B-29	Fir wood	Supported crib	Free burn	250	High/High	0.1-0.05	11.8	100	0.54	33	10.0
B-30	Fir wood	Supported crib	Free burn	250	High/High	0.077-0.034	13.0	120	No plug	19	4.2
B-31	Fir wood	Supported crib	Free burn	250	High/High	0.06-0.03	13.0	100	No plug	9	13.0
B-32	Kiln-dried fir wood	Supported crib	Free burn	250	High/High	0.12-0.03	14.8	112	0.31	34	3.0
B-33	Polycarbonate	Supported crib	Fusing sprinkler	250	High/High	—	4.5	70	No plug	—	—
B-34	Fir wood	Supported crib	Free burn	500	High/High	0.1	12.2	180	No plug	33	12.4
B-35	Fir wood	Supported crib	Free burn	500	High/High	0.085/0.054/0.035	18.9	180	No plug	0	25.0
B-36	Fir wood	Supported crib	Sonic cooling	500	High/High	0.097-0.058	15.0-11.0	140-75	0.64	8	16.2
B-37	Fir wood	Supported crib	500-l/s filter	250	High/High	0.085-0.42	12.2	105	No plug	30	19.2
B-38	Composite	Supported crib	Free burn	500	High/High	0.05	4.2	103	0.44	27	8.6

15th DOE NUCLEAR AIR CLEANING CONFERENCE

The rolling prefilter appeared* to offer the most promise as an active control since it can be used for a dual purpose; i.e., enhanced filtration** and HEPA fire protection. A passive control strategy might be to simply double the size of the HEPA relative to the design air throughput.

Scrubbing by in duct spray techniques did not increase filter lifetimes appreciably; in fact, there is some indication that the cooling effects of sprays may enhance the condensation of volatile aerosols, thus making plugging more likely. Fire control sprinklers effectively applied to the crib appeared to reduce the intensity of the fire and consequently the smoke production. In only one case did the HEPA plug after sprinkler application. The fuel was polycarbonate and the effect may be propitious.

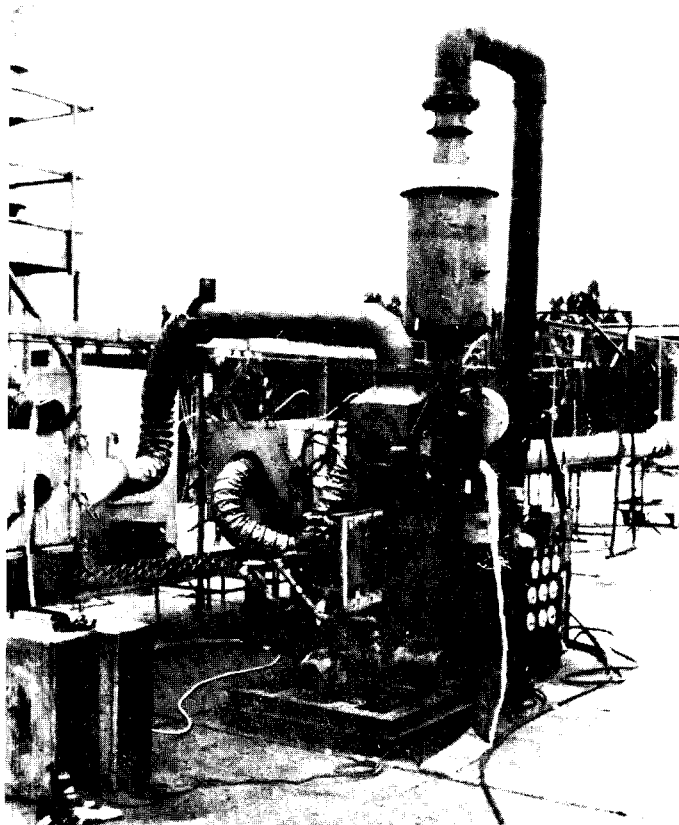


Fig. 6. Rolling prefiltration system installed in the LLL duct system.

IV. Summary and Conclusions

We have exposed HEPA filters to very severe smoke loads from potential fuel materials common in the furnishings and appliances of laboratories containing radioactive materials to identify and test practical filter plugging countermeasures before installing and retrofitting them in DOE facilities. Our tests indicated HEPA filters are inherently capable of handling huge aerosol concentrations

* In August of 1977, LLL rented a pilot model rolling prefiltration system and operator from the Anderson Corporation. The unit is generally used for filtration of air pollution aerosols and is based on high velocity trapping and scrubbing techniques. In our operations, we circumvented the scrubbing section. Figure 6 shows the unit installed in the LLL duct system. The HEPA was downstream from this unit.

** DOE's Enhanced Filtration Project is aimed at increasing the normal operational HEPA lifetime by unique prefiltration procedures.

TABLE V. Effect of various countermeasures on filter performance

Countermeasure	Fir wood		PMMA-FR		Polycarbonate		Dense fiberboard		Fiber-reinforced polyester		Polyvinyl chloride		Composite	
	t_{plug} , s	\dot{m} , kg/s	t_{plug} , s	\dot{m} , kg/s	t_{plug} , s	\dot{m} , kg/s	t_{plug} , s	\dot{m} , kg/s	t_{plug} , s	\dot{m} , kg/s	t_{plug} , s	\dot{m} , kg/s	t_{plug} , s	\dot{m} , kg/s
Free burn (enclosure)	320	0.12	400	0.03	No plug	0.04	No plug	0.08	880	0.02	590	0.02	400	0.02
Water scrubber (1-100 ℓ /min)	350	0.11												
Fusing sprinkler	No plug	— ^a	No plug	— ^a	550	— ^a	No plug	— ^a	No plug	— ^a				
Rolling prefilter	No plug	0.08											No plug	0.07
Wet wood	No plug	0.03												
Large HEPA surface	No plug	0.035												
^a For most fires, sprinklers activation occurs before steady-state burning.														

15th DOE NUCLEAR AIR CLEANING CONFERENCE

equal to the maximum rates from a flashed-over* room, however, the filters will ultimately plug. Attempts to control the fire by passive fire control sprinkler systems reduced the smoke load and generally the filter plugging potential of the aerosol. In the absence of a fire control system, prefiltration techniques appeared to hold a promising means of increasing filter endurance under extreme aerosol exposures. The simple expediency of doubling the filter size relative to the design flow rate of the ventilation system also appeared promising as a passive smoke aerosol countermeasure.

So far, none of our filters have been thermally damaged since the heat lost to the duct was sufficient to reduce the temperature of the combustion products to safe levels ($T_{\text{gas}} \leq 180^\circ\text{C}$). However, at gas temperatures greater than 120°C , some volatile components of the combustion products passed through the filter and condensed downstream. We are uncertain if this is a compromise of containment.

We are currently analyzing the chemical components of smoke aerosols responsible for filter plugging. Our gross physical measurements indicate that most fuels tested thermally degrade to specific aerosol mixtures that contain effective filter plugging components. Our efforts in this area will continue at a reduced rate since we intend to concentrate on practical countermeasure techniques unless we can identify a super and universal filter plugging component of all aerosols.

Our future efforts will be directed toward optimizing rolling prefiltration procedures and toward providing scaling guidelines for the inclusion of rolling prefilters in any size containment system.

V. References

1. J.R. Gaskill, N.J. Alvares, D.G. Beason, and H.W. Ford, "Preliminary Results of HEPA-Filter Smoke Plugging Tests Using the LLL Full-Scale Fire Test Facility," Lawrence Livermore Laboratory, Rept. UCRL-77779, (Aug 2-4, 1976).
2. J.A. Block, "A Theoretical and Experimental Study of Nonpropagating Free-Burning Fires," 13th Symposium (International) on Combustion, pp 971-978, The Combustion Institute, (1971).
3. W.J. Parker, "An Investigation of the Fire Environment in the ASTM E-84 Tunnel Test," NBS Technical Report, pg 945, (Aug 1977).
4. A. Pompe and R.G. Vines, "The Influence of Moisture on the Combustion of Leaves," Australian Forestry, Vol. 30, No. 3, (Sept 1966).

* In this paper we define "flash-over" as the condition when all combustible items in an enclosure are involved in fire.

15th DOE NUCLEAR AIR CLEANING CONFERENCE

DISCUSSION

FREEMAN: I served on an ANSI committee which wrestled with the question, "When is a filter plugged?" Could you give me your rationale for the definition of plugged filter that you define as "When the flow rate is reduced by half"?

ALVARES: We grabbed it out of the air. It appears that when a filter gets to half of the design flowrate it is accelerating to a plugging mode at a very fast rate. It's simply arbitrary.

BURCHSTED: A further comment on this point; earlier results of a program in which filters were totally plugged (i.e., airflow went to zero) showed that time to total plugging was very rapid after airflow dropped to 50% of normal system flow. The value of 50% of flow must be 50% of system flow, not 50% of filter element design flow. A recommended practice for fire/smoke alleviation is to operate filter systems at 50% of nominal filter flow. Plugging, in this case, would be 25% of filter airflow capability.

15th DOE NUCLEAR AIR CLEANING CONFERENCE

AIR CLEANING SYSTEM ISOLATION DURING TORNADO CONDITIONS

W. A. Pysh & T. A. Clements
Techno Corporation
Erie, Pennsylvania

Abstract

The occurrence of a tornado at the site of an operating nuclear power generating station creates unstable atmospheric conditions which can be detrimental to the proper operation of the plant air cleaning system. One means of mitigating or preventing this hazard is isolation of the system from the unstable environment by closure of the system openings during the unstable conditions. For maximum system protection the closure should be an automatic response to the adverse conditions themselves, without reliance on manual or remote sensing or signals.

The interaction of tornado characteristics with velocity/pressure sensitive isolation devices is modeled. Force and time relationships are investigated to evaluate and predict the interaction. Laboratory test apparatus is developed for simulating the flows and pressures induced by the tornado at system openings. Several isolation devices of various sizes are subjected to a range of simulated tornado conditions for observation and evaluation of response time, sensitivity, and dynamic closing forces. The model, apparatus, experimentation, and results are presented.

I. Introduction

It has become commonplace in recent years to protect nuclear power plant air cleaning systems from the effects of tornado induced flows and pressures by means of isolation valves or dampers which close automatically in response to those potentially damaging flows and pressures.

The justification for providing this protection may be based on the requirements of Regulatory Guide 1.117, "Tornado Design Classification", to control the release of radioactive materials and to provide for the safe shutdown of the plant; or on engineering economic analysis of the cost of protection versus the probability of the cost of repair or replacement of system components.

Current practice has been away from "administrative" control of isolation; that is, procedurally controlled manual or remote operation of shutoff devices, and toward the use of valves and dampers which close in direct response to the tornado induced flows or pressures. The effectiveness of such devices depends upon how quickly they respond to the tornado induced conditions, and to what extent this response limits the effect of those tornado induced conditions on the system components.

15th DOE NUCLEAR AIR CLEANING CONFERENCE

It is the purpose of this study to attempt to begin to answer those questions. The laws of fluid mechanics shall be utilized to model and understand the interaction of the various devices with normal and tornado induced system flows and pressures. Tests will be performed to verify the validity of the model selected. Finally, system effects will be evaluated with isolation devices in place and compared to system effects with no isolation from tornado induced conditions.

II. Design Basis Tornado

Regulatory Guide 1.76, "Design Basis Tornado for Nuclear Power Plants" gives the characteristics for the Design Basis Tornado that must be considered by the system designer. For background in the development of this tornado model, the reader is directed to the several references listed. (2) (6) (7)

Those characteristics which have potentially damaging effects on the air cleaning systems are the high rotational and translational winds at the tornado perimeter (624 km/hr, 360 mph) and the very rapid drop in atmospheric pressure within the tornado vortex, (20.7 kPa, 3 psi, in 1-1/2 sec). These changes in ambient conditions are very short lived but take place very rapidly. For this reason, any device which is to provide protection from these conditions must be very responsive.

The possibility of very high winds at the perimeter and uncompensated deficits in the vortex, combined with the possible occurrence at either supply or discharge openings, presents a matrix of system effects which are shown in Table I.

Table I. System Effects

	Supply Openings	Discharge Openings
High Winds	Surges in	Reversal
Vortex Deficit	Reversal	Surges out

III. Isolation Devices

Protection against reversal is provided by the use of appropriately designed check valves or back draft dampers. Normally such devices have some mechanism, such as springs or counterweights, which initiate motion toward closure before actual reversal occurs.

Protection against surges is provided by means of velocity/pressure sensitive devices which allow flows in the normal operating range, but which close when above normal flow rates are encountered. This sensitivity is provided by a mechanism, such as a trip latch,

15th DOE NUCLEAR AIR CLEANING CONFERENCE

spring, or counterweight, which holds the valve or damper open against the forces imposed by normal operation, but which is overpowered by the forces of excessive flow rates or pressure differentials, allowing, or causing the device to close.

Valves and dampers for this application may rely on different mechanics of interaction with the flow stream. Figure 1 shows a device with two separate centrally pivoted, totally unbalanced blades, which rotate in opposite directions to close. This device, identified as "Wing Blade" type in ANSI N509, operates from the transfer of stagnation pressures developed in the apex of the two blades to provide closing moment.

Figure 2 shows the damper in a closed position, isolating the system downstream.

For all types normal flows will cause a closing force which is resisted by the aforementioned mechanisms. However, once the normally expected range of these flows is exceeded, the devices move very rapidly to a closed position, isolating the system from further effect.

While it is quite common for tornado isolation devices to be mounted in ducts, with flow orientation either horizontal or vertical, a more typical installation is that of plenum mounting with missile barrier protection. Such an installation is shown in Figure 3.

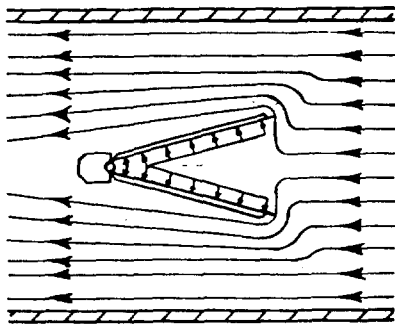


Figure 1 Wing Blade
Damper - open

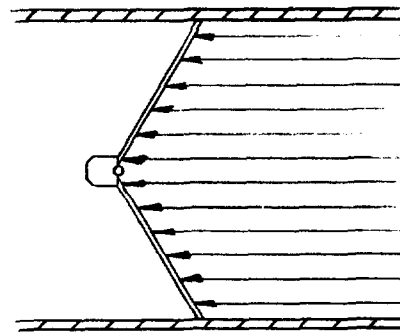


Figure 2 Wing Blade
Damper - closed

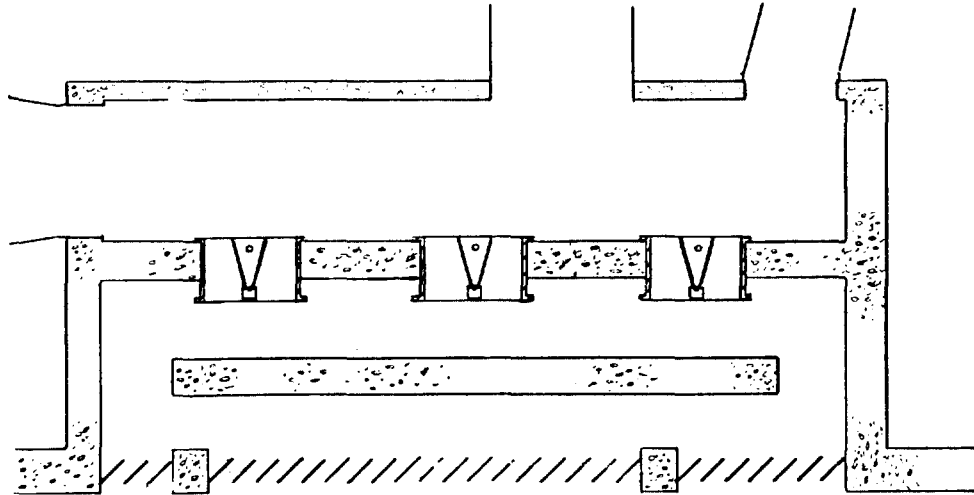


Fig. 3 Typical installation

IV. Analytical Model

A wing blade damper forms an obstruction in a flow path and, as such, can be analyzed from the mechanics of flow about an immersed object. (Figure 4) A pressure differential $P_0 > P_2$ will cause a flow to take place which will impinge on the upstream face of the obstruction, developing a stagnation pressure within the apex of the blades. For the flows and pressures of normal air cleaning system operation this pressure will be equal to the total pressure of the impinging air stream, TP_0 .

As the flow continues around the obstruction, there will be a loss of energy through the combination of eddy formation at the blade edges and friction loss along the downstream, or backblade surface. As the profile of the obstruction increases relative to the flow area (Figure 4b) the loss due to eddy formation will predominate, with most of the loss taking place at the blade edges.

If the blades are free to rotate about a hinge at the apex, which is the case for the wing blade damper, the stagnation pressure acts to move the blades in the direction of flow, while the static pressure distribution on the back side of the blades opposes this motion.

Given these flow induced forces, and the existence of gravity forces on the blades in vertical flow installations, the blades can be made to respond in a controlled manner to changes in the flow conditions by the addition of mechanisms which produce forces of known magnitude and direction, such as the previously mentioned latches, springs, or counterweights.

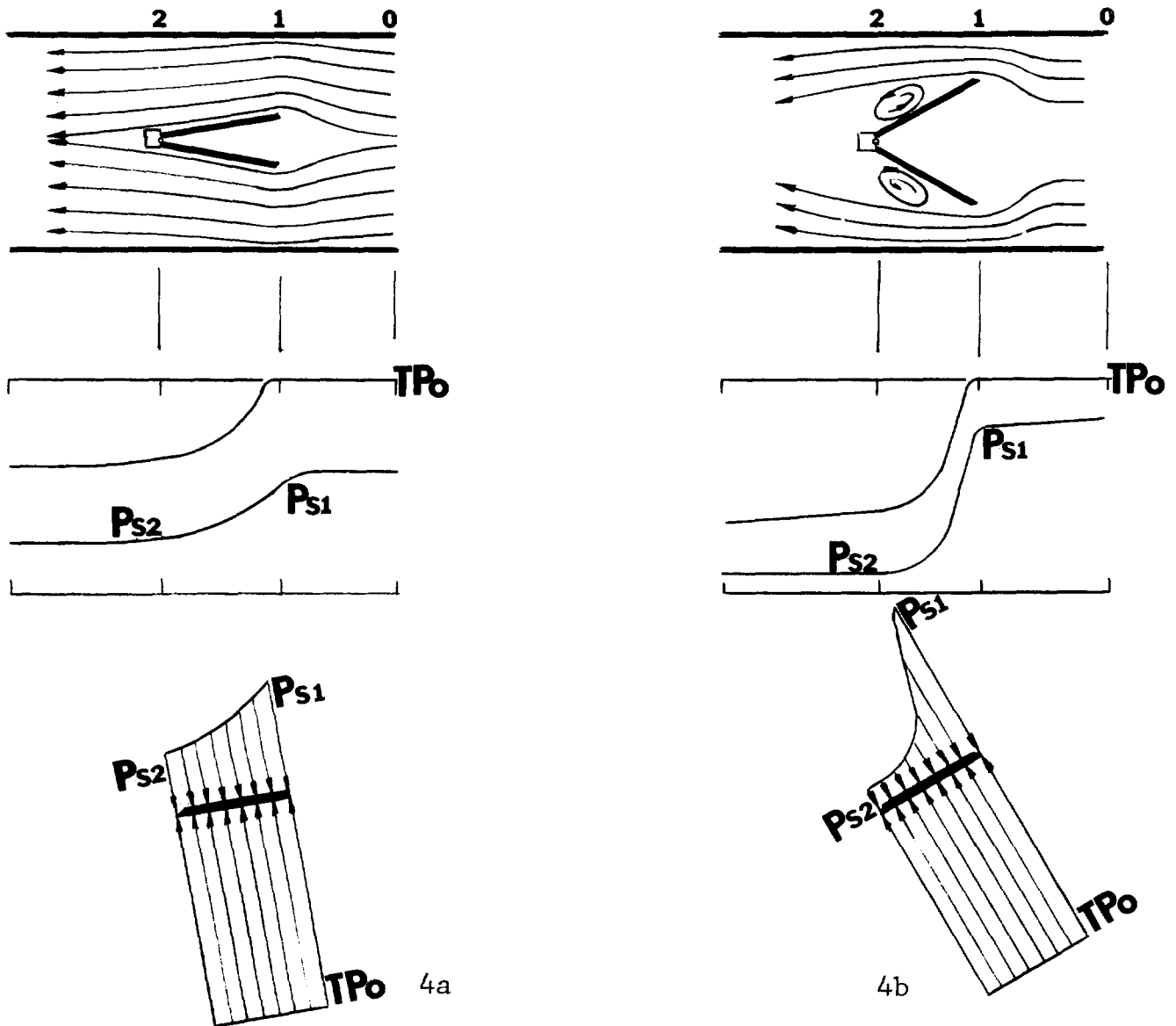


Figure 4. Flow lines, pressure gradients, and free body diagrams - duct flow

For example, if a force were added to Figure 4a equal to $-(TP_0 - \sum P_s)$ the blades would be in equilibrium, allowing flow from $P_0 > P_2$ to take place, as in normal operation. If $P_0 > P_2$ flow were vertical upward, gravity action on the blades would provide this force. As another example, if initial flow were $P_2 > P_0$, with the tornado causing a reversal to $P_2 < P_0$, a force could be added to initiate closing action before reversal occurred.

The resultant of all of these forces causes a moment which is given by:

$$M_R = (TP_0 - \sum_{P_{s1}}^{P_{s2}} P_s) A \bar{X} \pm M_G \pm M_F \quad (1)$$

Where M_G is the moment caused by gravity forces and M_F is the moment caused by the controlling forces F .

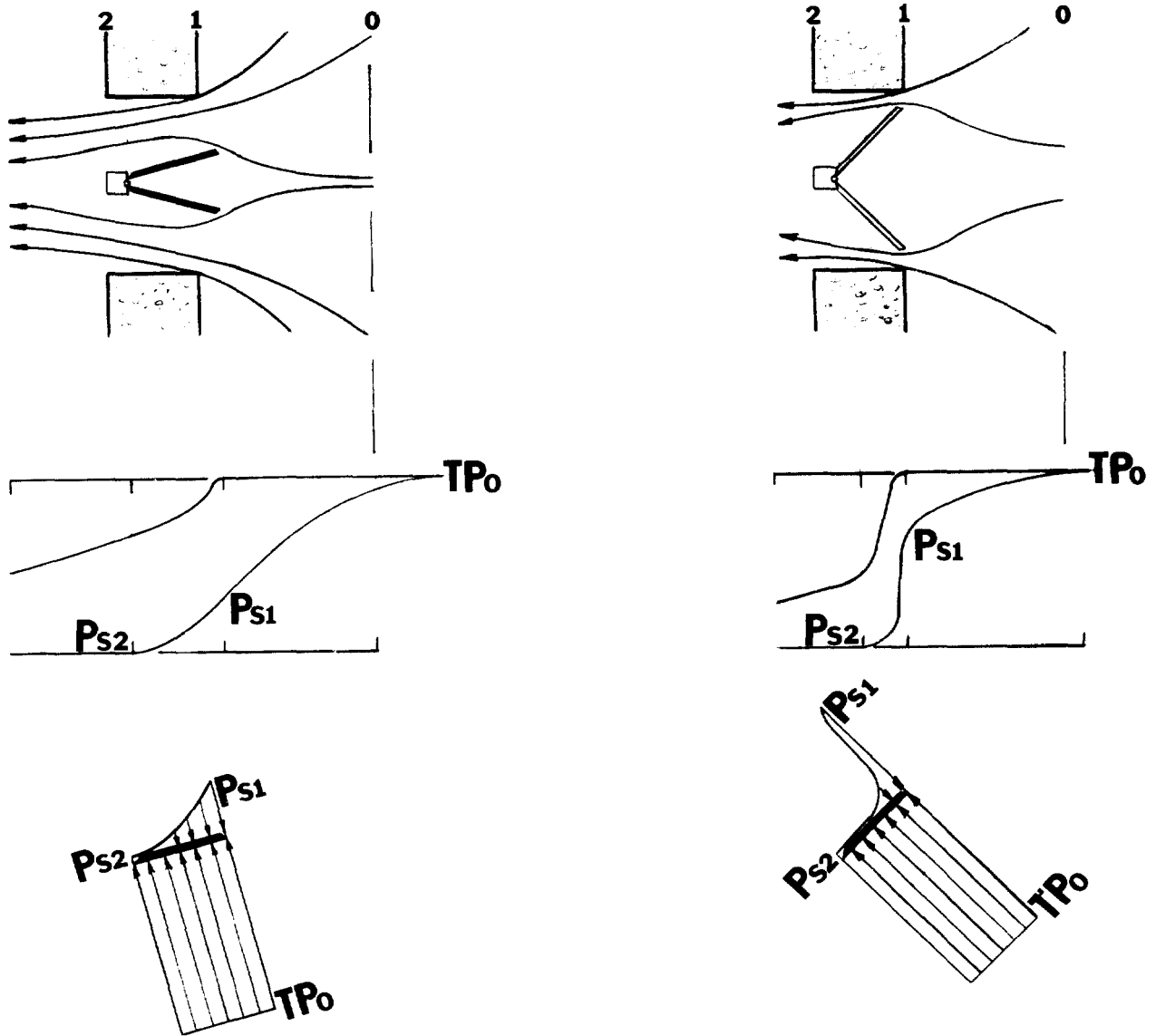


Figure 5. Flow lines, pressure gradients, and free body diagrams - orifice flow

Since A , \bar{x} , M_C and M_F are all known for a given application, it remains to determine the flow and pressure transients to which the isolation device must respond to provide the required protection. If an accurate and reliable analysis of the tornado effects on the entire system is available, the degree of protection required and the location of the protective devices will become apparent. Since such an analysis may not be readily obtainable, it may be possible to determine the maximum allowable transients by an evaluation of the limitations of the downstream components, such as filters.

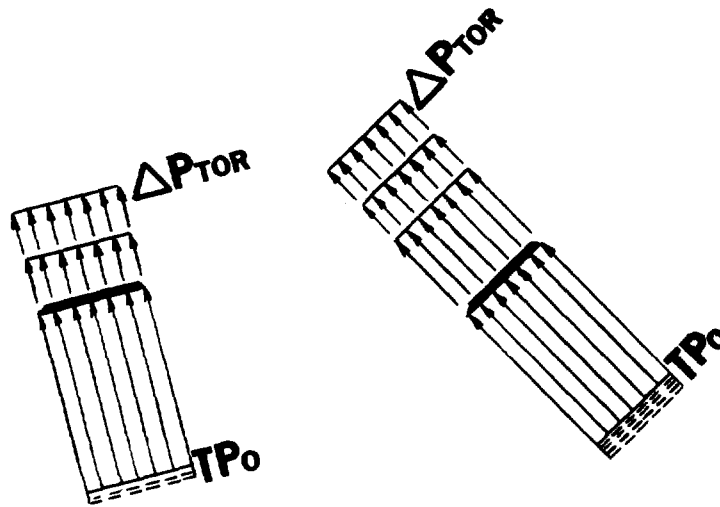


Figure 6. Assumed free body diagrams
orifice flow - during tornado pressure drop

More commonly, however, the decision is made to install the isolation valves and dampers as the first and last components in the system, and to require that they respond directly to the atmospheric conditions of the tornado. While this simplifies the transient solution, it is still necessary to evaluate the time rate of change of the normal system flows and pressures at the inlet and outlet openings.

Fortunately it is very common to have plenums at these openings, and this allows simplifying assumptions to be made. Such a case is essentially that of orifice flow between two large volumes. (Figure 5) For flow through an orifice the major energy loss occurs after the Vena Contracta, and therefore the total energy in the flow stream at (1) is equal to the total (static) pressures at (0) where the velocity is very low. For a wing blade damper located in the orifice, the stagnation pressure in the apex will be equal to the static pressure in the plenum for all normal flow rates. The static pressure distribution $\sum P_s$ will be small relative to TP_0 .

As a tornado induced drop in pressure P_2 occurs, the pressure distribution can be assumed to be that given by the Design Basis Tornado. If the storage capacity of the plenum is sufficient, outflows will have little effect on the static pressure for the short time interval involved and TP_0 can be assumed fixed (Figure 6).

Therefore, if $\sum P_s$ is assumed to be $\Delta P = f(t)$ and TP_0 is assumed constant, with other factors in equation (1) known, the motion of the blade can be defined.

It is this special case of orifice flow from a plenum that will form the basis for the first phase of the testing.

V. Testing

Static Tests

The first phase of testing consisted of utilizing existing laboratory apparatus to verify the static pressure relationships assumed in the model. The apparatus (Figure 7) is essentially that described in AMCA Standard 500-75, "Test Method for Louvers, Dampers, and Shutters."⁽⁸⁾ By varying the position of the control damper to establish "fan" curves and the position of the test damper blades to establish system resistance curves, a family of fan-system curves was created. (Figure 8)

At each point data was collected as shown in Figures 7 and 9. Data collection and adjustment procedures were as given in the AMCA 500 Standard. The force (F , Figure 9) was taken from a force gage connected to the test damper blade. All data was used directly except that the flow was determined by the P_v values at the pitot tube traverse, and the measured closing moment on the blades (M_{meas}) was calculated from a , F , and β .

The test chamber was a cube measuring 3.2 m (10 ft.) on a side, and the test damper was a 1.15 m (42 inch) wing blade damper, equipped with a trip latch which was capable of adjustment for release at varying flow rates. This arrangement was representative of a surge protection device located in a discharge plenum. Increases in flow rates would act to overcome the trip latch and cause closure.

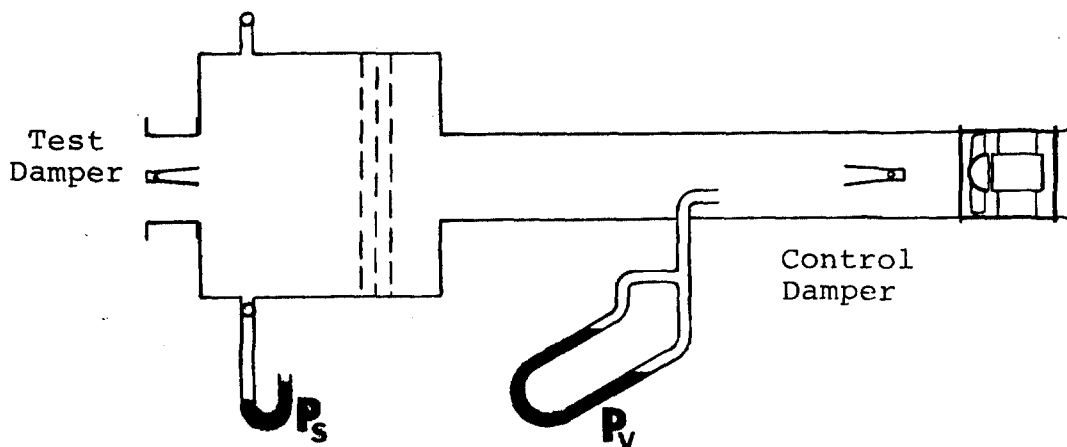


Figure 7 Test Apparatus

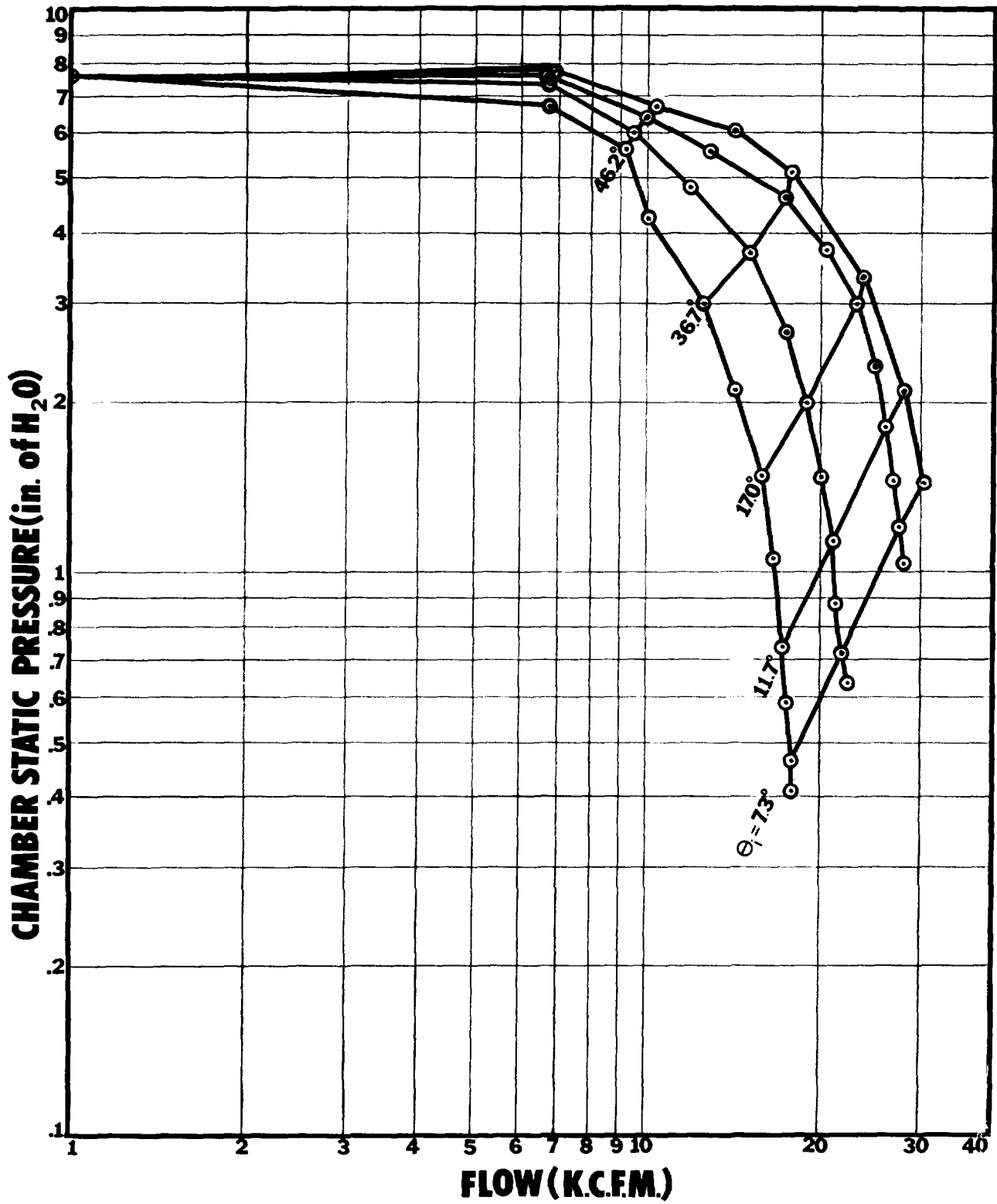


Figure 8 Fan-system resistance curves

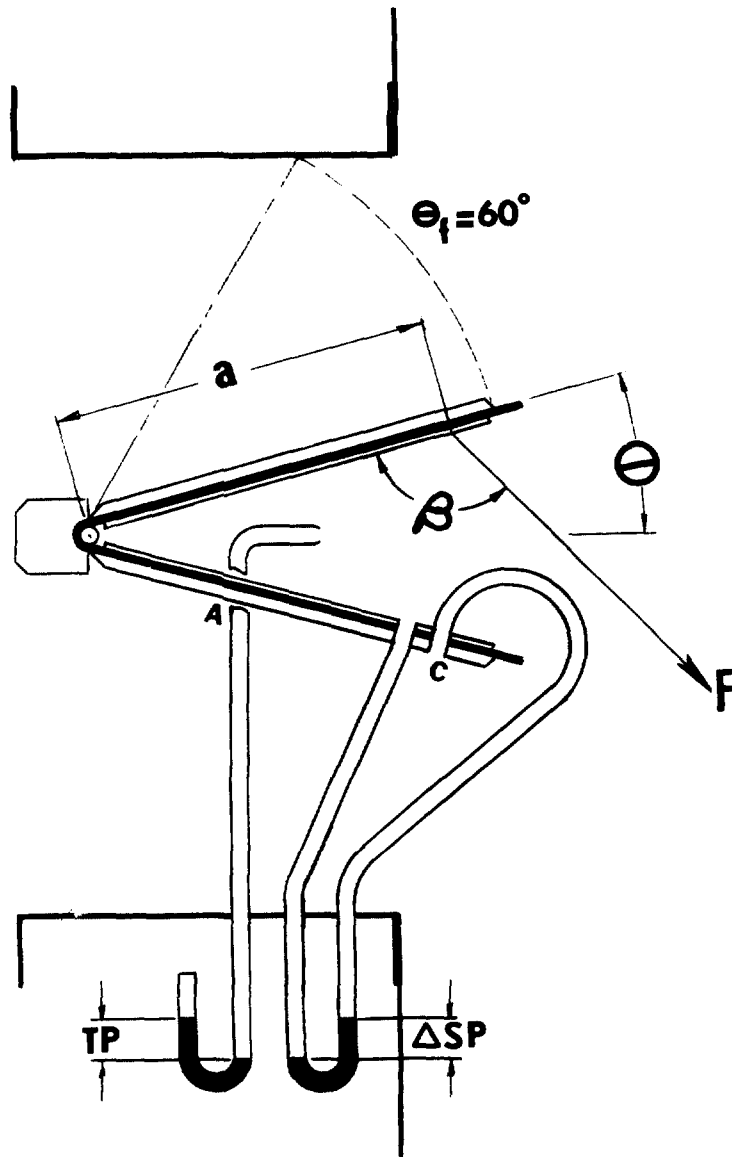


Figure 9 Data Collected

Verification of the assumed model for this arrangement consisted of comparing (1) the static (total) pressure in the chamber (P_S) with the stagnation pressure measured in the apex of the blades (TP) (2) the relationship between the unbalance pressures on either side of the blade at two locations (ΔSP_A , ΔSP_C); and (3) the closing moment calculated from the stagnation pressure (TP) alone acting on the blades (M_{calc}) with the measured moment (M_{meas}).

A comparison of TP and P_S at all data points showed the two values to be equal in all cases, with a maximum deviation of 0.02 inches W.G. The conclusion is that, for the arrangement and flow ranges included, the stagnation pressure in the apex of the blades was equal to the chamber static (total) pressure.

15th DOE NUCLEAR AIR CLEANING CONFERENCE

Comparing ΔSP_A and ΔSP_C gives an indication of the static pressure profile on the downstream surface of the blades. It would be expected that the ratio $\Delta SP_C / \Delta SP_A$ would be small for a more open blade, where some friction drag would occur along the back blade surface, and would increase as the blade angle increased, when separation would occur at the blade edge. These expectations were confirmed by the data (Table II).

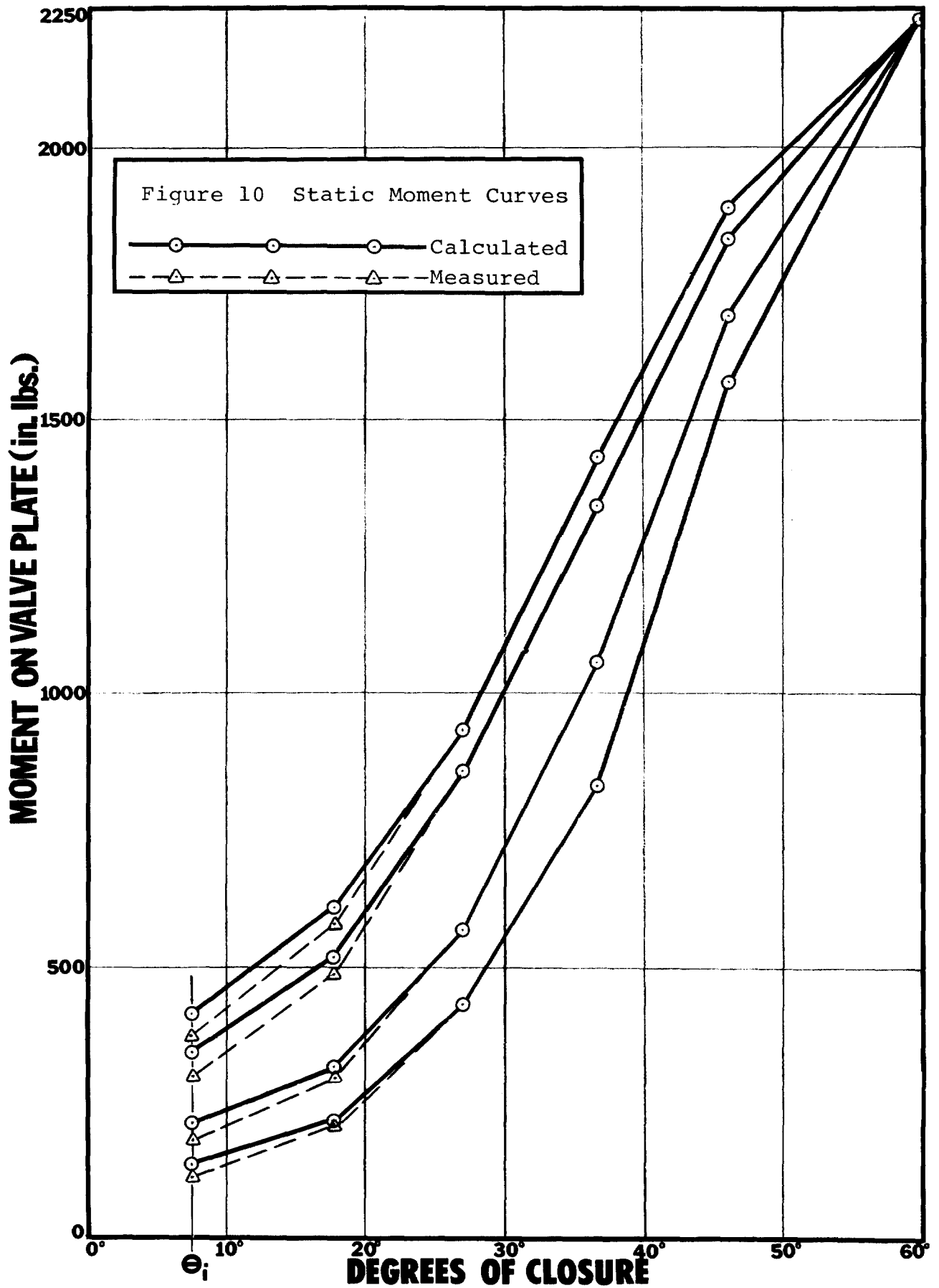
Table II. Pressure profile on back blade surface

Blade Position	$\frac{\Delta SP_C}{\Delta SP_A}$	Maximum Deviation
7.3°	.34	.02" W.G.
11.7°	.46	.01
17.0°	.67	.04
36.7°	1.00	.02
46.2°	1.00	.03

It is interesting to note here that, for a given blade setting, there was no significant change in the back surface profile within the flow ranges of the test series.

The final comparison to be made for the static model is between M_{calc} and M_{meas} . The model assumes for this arrangement, i.e., plenum flow to atmosphere, that the only significant force acting to close the blade is the apex pressure on the inside blade surface. This force would create a moment which is calculated from TP and blade geometry to give M_{calc} . The model acknowledges a static pressure distribution on the back surface but concludes that its effect is insignificant. The difference between M_{calc} and M_{meas} in the testing represents the significance of the back surface pressure distribution, and therefore, the suitability of the model assumption.

The results of the comparison (Table III, Figure 10) seem to substantiate the model assumption. While there is some variation shown at more open blade positions, the difference becomes very small with little blade movement.



15th DOE NUCLEAR AIR CLEANING CONFERENCE

Table III. Blade Moments

Blade Position	$\frac{M_{meas}}{M_{calc}}$ (range)
7.3°	.85 to .93
11.7°	.94 to .99
17.0°	.98 to 1.04
36.7°	.96 to .99
46.2°	not available

Closing Time Tests

The same test apparatus was used to obtain closing times for the test damper when subjected to several different flow conditions. These closing times were then compared to that which would be expected from a quasi-static application of the damper model to those same flow conditions.

The experimental closing times were generated by setting the trip latch to release at a previously defined flow and measuring the travel time from release to closure by means of an electronic clock controlled by switches at the release and closure positions.

By setting the trip latch to release from the position θ_i , at the flow rate previously established for that position on each of the four fan curves used in the static test, the initial conditions of motion are given. The quasi-static assumption is that, as the blade moves toward the closed position, the flow will be governed by the fan curve, and the intersections of the fan-resistance curves will define the pressure relationships at that point.

The test apparatus and procedure give the pressure relationships as a function of position, rather than time, as would be the case for the Design Basis Tornado. However, the $M = f(\theta)$ data (Figure 10) is available to provide the time relationship.

The equation of motion for the blades is that of a mechanism rotating about a fixed point in one plane, and as such, is given by:

$$I_o \ddot{\theta} = M \tag{2}$$

For the quasi-static solution it is assumed that:

$$M = f(\theta) = K\theta + M_i \tag{3}$$

15th DOE NUCLEAR AIR CLEANING CONFERENCE

Where K is the slope of the $M = f(\theta)$ curve and M_i is the moment at the trip point θ_i .

Combining equations (2) and (3) gives:

$$I_0 \ddot{\theta} = K \theta + M_i \quad (4)$$

The general solution to this 2nd order differential equation is given by:

$$\theta = C_1 \cosh \left[\frac{K}{I_0} \right]^{\frac{1}{2}} t + C_2 \sinh \left[\frac{K}{I_0} \right]^{\frac{1}{2}} t - \frac{M_i}{K} \quad (5)$$

Therefore, given θ as the angle traveled to closure, K and M_i for the several fan curves (Figure 10), and I_0 for the test damper, the predicted closing time, t_{calc} , can be determined.

The results of the comparison of predicted closing times (t_{calc}) and measured closing times (t_{meas}) for the test series (Table IV) indicates that the procedure used gives a reasonably reliable prediction of closing time.

Table IV. Closing Time

Trip Velocity	t_{calc} (seconds)	t_{meas} (seconds)
9.5 m/s (1870 fpm)	.29	.24
		.25
		.24
11.6 m/s (2290 fpm)	.24	.20
		.19
		.20
14.8 m/s (2920 fpm)	.19	.16
		.16
		.16
16.2 m/s (3190 fpm)	.18	.16
		.16
		.16

VI. Conclusion

The use of automatic isolation devices to protect air cleaning systems from the effects of a tornado requires that these devices respond very quickly to the large, rapid, and short lived changes in atmospheric conditions that occur.

In the absence of a history of experience of plant reaction to tornado effects, the knowledge of behavior of the valves and dampers in response to the tornado induced transient must come from analytical and experimental effort.

Techniques are available for analytical solution of the equations of motion of the devices used, and also for determining the transient conditions within the system. The laboratory simulation of conditions imposed by a real tornado presents a considerable obstacle to experimental work in this area, however, some beginnings are underway.

From the work to date, it can be concluded that very rapid closure times are achievable. As an example, a wing blade damper, similar to the one used in the test, but of heavier construction, when mounted in plenum, discharging horizontally to atmosphere at 9.5 m/s (1870 fpm), and subjected to a 13.8 kpa/sec (2 psi/sec) atmospheric pressure drop, will close in 0.23 seconds, with a final angular velocity of 13.3 radians/sec. During the time of closure the total drop in atmospheric pressure would have been 3.45 kPa (0.5 psi).

This rapid closure response, and resultant reduction in system exposure to the unstable atmospheric conditions, provides the required protection to internal system components.

VII. Effect of Isolation

The predictability of response times has value only if it aids in the evaluation of system effects. There are two possible avenues for this evaluation.

One would be to design and construct a physical scale model of the system to be analyzed and impose a physical simulation of a tornado upon it. Using appropriate similarity and dimensional analysis techniques, the system effects could be evaluated.

Another approach would be to create a mathematical model of the system and impose a tornado simulation in like manner. A means to accomplish this exists in the form of a computer program developed at the Los Alamos Scientific Laboratory. This program, TVENT, has been designed for the specific purpose of modeling HVAC system interaction with events such as tornados. (1) (3) (4) (5)

15th DOE NUCLEAR AIR CLEANING CONFERENCE

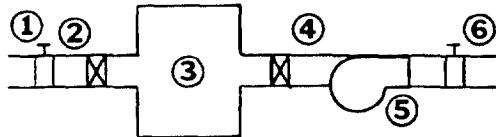
For purposes of illustration, TVENT was used to model a tornado interaction with a very simple system to observe the effects on the system with no isolation devices in place, and then again with isolation occurring.



The model system is shown in Figure 11, and the design basis tornado is shown in Figure 12. It should be pointed out at the outset that dramatic system effects are to be expected because the system is very small, with little natural attenuation, such as missile barriers and duct bends; and with very little system storage, so that small outflows will cause large pressure changes. Also it is to be noted that the tornado model used did not include the high winds surrounding the vortex.

Figures 13, and 14 show the system pressures and flows respectively with the DBT imposed at the system outlet.

For comparison purposes the program was repeated, this time using a controlled closure valve at node 5. The closing time was arbitrarily set at 0.5 seconds, with the resistance-time function as shown in Figure 21. The program instituted valve closure at a point when normal velocity was exceeded by 50%. The system effects for this condition are shown in Figures 15 and 16. Obviously there is a significant reduction in the pressures and flows encountered.

The above process was repeated with the DBT at the inlet with results shown in Figures 17 and 18 for no isolation, and Figures 19 and 20 with a check valve at node 1 to prevent reversal. The valve was instructed to prevent further flow once inlet flow value became negative. However, as the ambient pressure restored, the valve opened to allow positive flow once again. This action explains the very sharp increases around $T = 6$ seconds. It would not be unreasonable to expect such an action in a real system.



 Filter
 Valve

$Q_1 = 500 \text{ cfm}$
 $\text{Vol. 3} = 10,000 \text{ ft.}^3$

Fig. 11 Model system

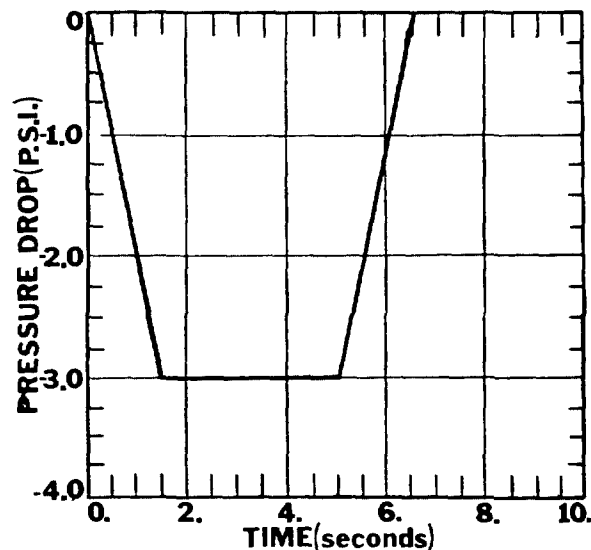


Fig. 12 Pressure Transient

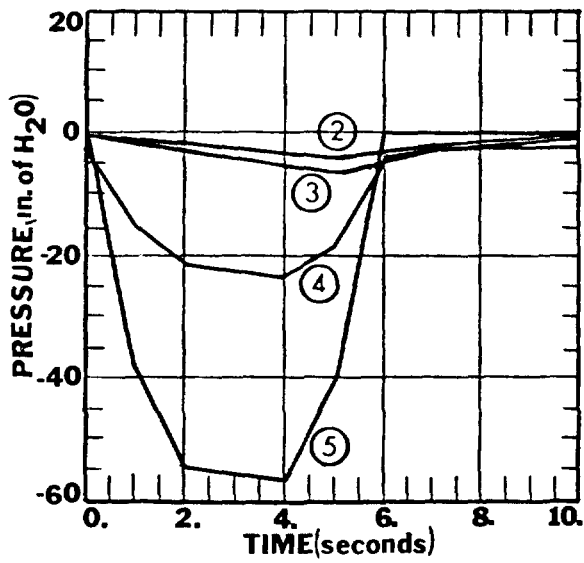


Fig. 13 System pressures - tornado at outlet

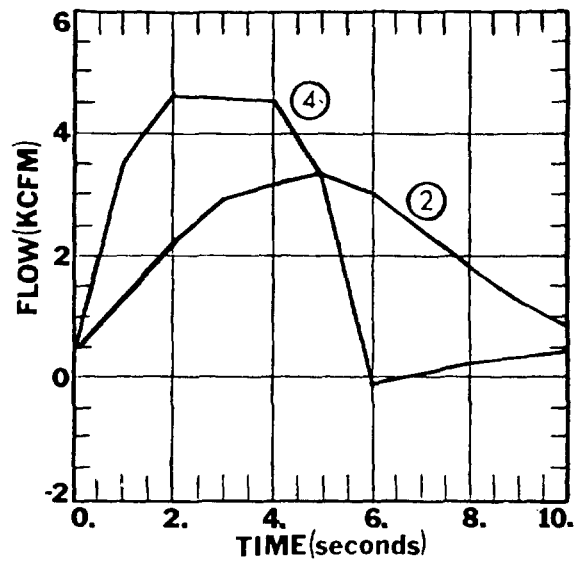


Fig. 14 System flows - tornado at outlet

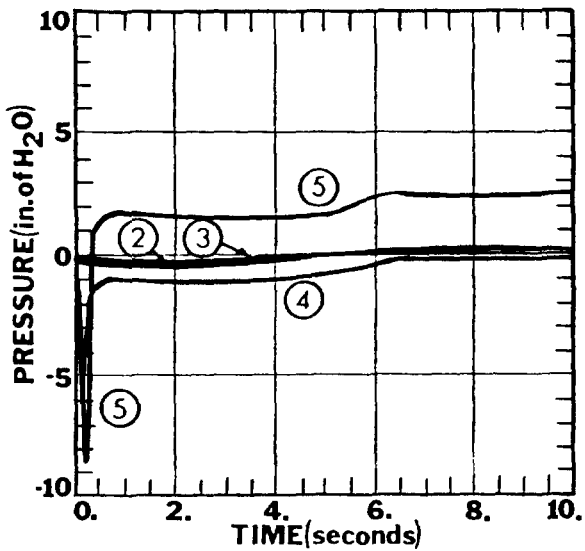


Fig. 15 System pressures - tornado at outlet with isolation valve

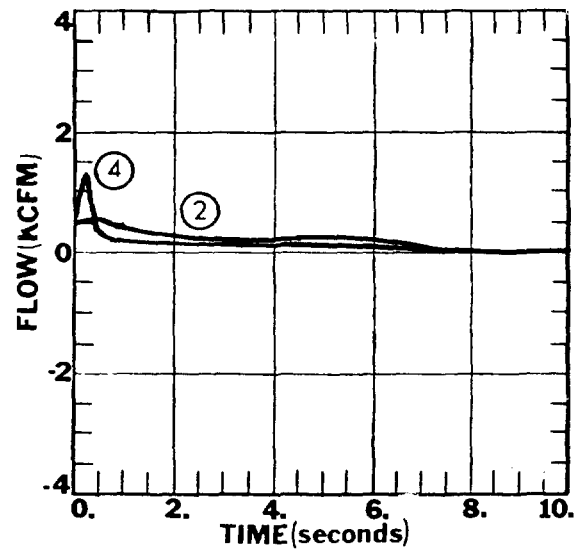


Fig. 16 System flows - tornado at outlet with isolation valve

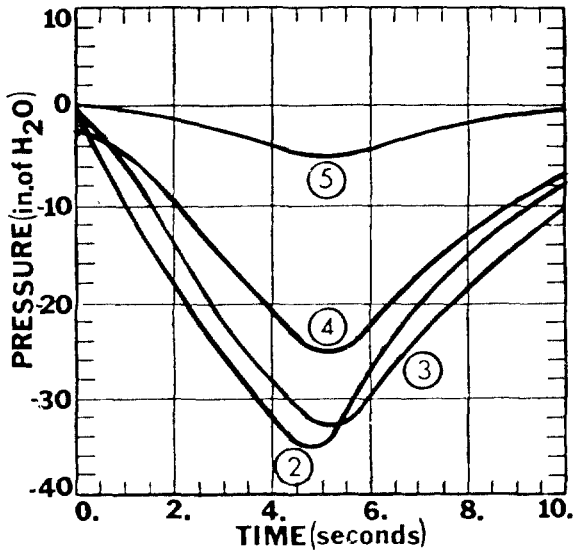


Fig. 17 System pressures - tornado at inlet

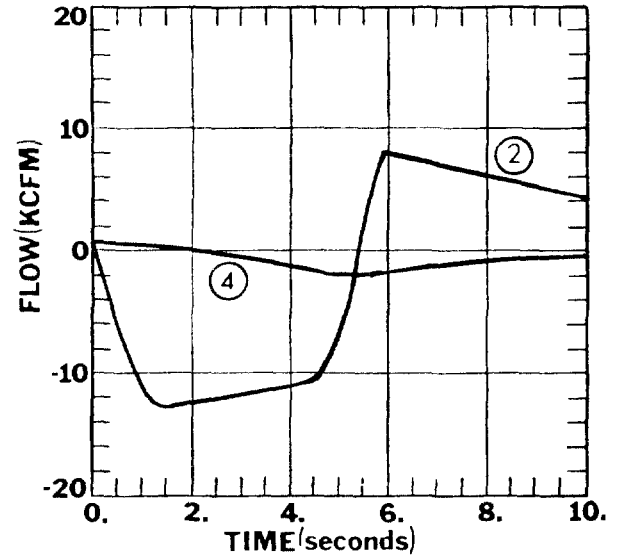


Fig. 18 System flows - tornado at inlet

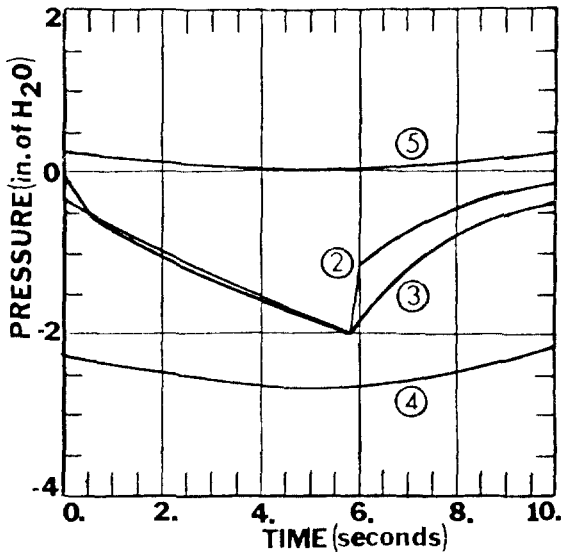


Fig. 19 System pressures - tornado at inlet with isolation valve

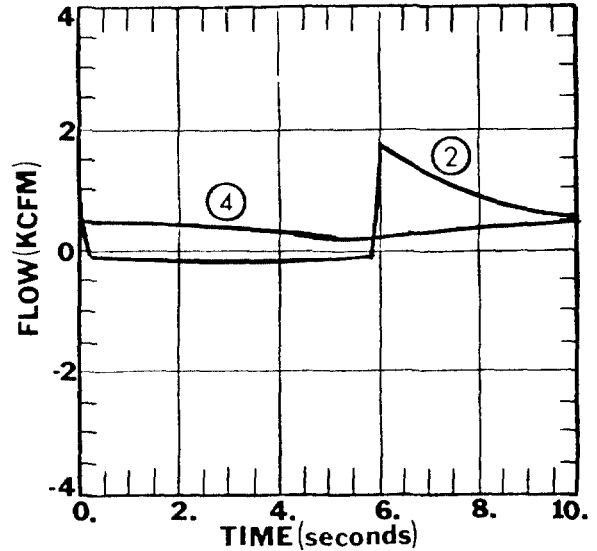


Fig. 20 System flows - tornado at inlet with isolation valve

15th DOE NUCLEAR AIR CLEANING CONFERENCE

Real life systems are enormously more complex than the simple system model chosen, and have some built in attenuation provided by normal system construction. However, this example does illustrate two points. The first is to confirm the intuitive, if qualitative, reasoning that isolation will have positive effect in reducing expected system flows and pressures. Secondly, it provides evidence that a method of quantifying that effect is currently available.

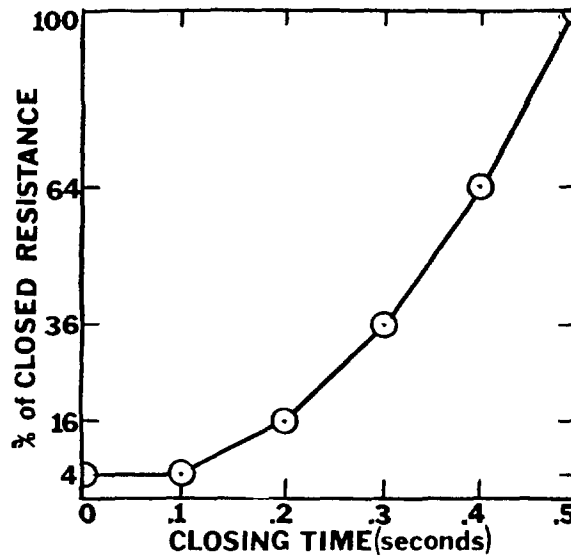


Fig. 21 Resistance curve for outlet control valve

VIII. Future Effort

The goals of this project as originally stated were to (1) devise a suitable model for the isolation device to allow predictability of responses, (2) design and carry out sufficient testing to verify the validity of the model, and (3) use the predicted response to evaluate the protection provided to real systems.

To this end the following remains to be accomplished:

1. The product model shall be refined to more closely approach real system conditions by the inclusion of dynamic relationships.

15th DOE NUCLEAR AIR CLEANING CONFERENCE

2. Testing shall be carried out under conditions which more closely simulate the Design Basis Tornado. Apparatus for this testing is being developed and is shown schematically in Figure 22. The pressure wave will be simulated by rupturing a disc on the high pressure storage tank, releasing a controlled pulse down the duct to impact with the test valve. Time-pressure readings will be obtained from pressure transducers providing a signal to a time controlled trace. Physical behavior and closing times will be monitored by high speed photography.

3. The LASL TVENT program will be used to analyze and evaluate real systems with and without isolation protection.

4. System effect caused by the rapid closure must be considered in the model, testing, and evaluation. Such effects might include shock wave generation, motor loading of fans and blowers, and duct starvation.

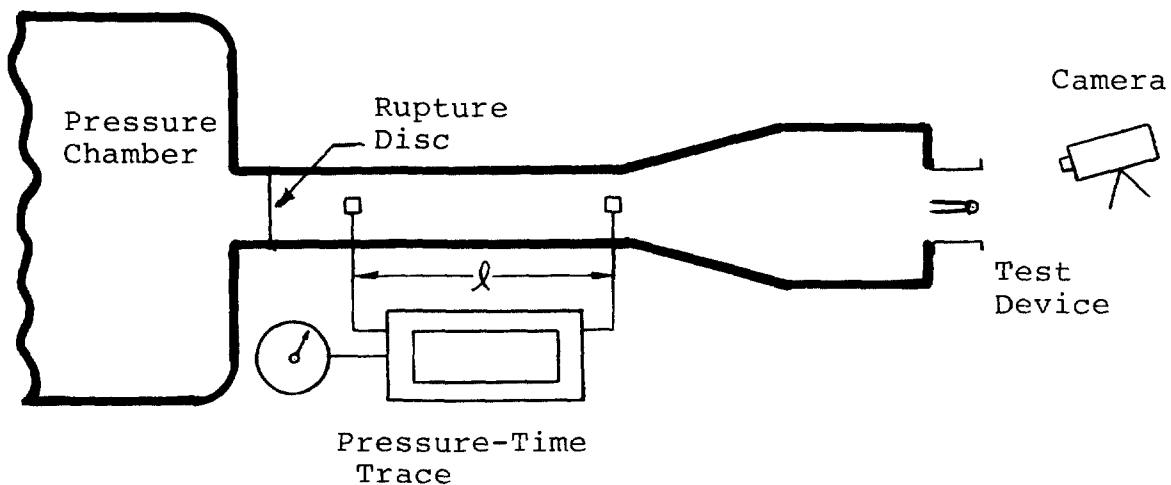


Figure 22 Proposed Test Apparatus

15th DOE NUCLEAR AIR CLEANING CONFERENCE

References

1. Bennett, G. A., Gregory, W. S., Smith, P. R., Ventilation Systems Analysis During Tornado Conditions - January - June 1975, LA-6120-PR, Los Alamos Scientific Laboratory, Nov. 1975.
2. Doan, P. L., "Tornado Considerations for Nuclear Power Plant Structures", Nuclear Safety, July - August 1970.
3. Gregory, W. S., Bennett, G. A., Ventilation Systems Analysis During Tornado Conditions - July through December 1974, LA-5895-PR, Los Alamos Scientific Laboratory, March 1975.
4. Gregory, W. S., Duerre, K. H., Smith, P. R., and Andrae, R. W., "Tornado Depressurization and Air Cleaning Systems", Proceedings, 14th ERDA Air Cleaning Conference, NTIS No. Conf. 760822.
5. Gregory, W. S., Smith, P. R., Duerre, K. H., "Effect of Tornados, on Mechanical Systems", Proceedings Symposium on Tornados, Lubbock, Texas, 1976.
6. Markee, E. H. Jr., Beckerley, J. G., Sanders, K. E., Technical Basis for Interim Regional Tornado Criteria, U.S. Atomic Energy Commission Office of Regulation, Wash-1300, 1974.
7. McDonald, J. R., Mehta, K. C., Minor, J. E., "Tornado-Resistant Design of Nuclear Power-Plant Structures", Nuclear Safety, July - August 1974.
8. _____, "Test Method for Louvers, Dampers, and Shutters", AMCA Standard 500-75, Air Movement and Control Association, 1975.

DISCUSSION

MOELLER: Your map of tornadoes shows that the majority move in a northeasterly direction. Does this have any implications relative to the orientation of air intakes and exhausts in nuclear facilities?

PYSH: It has, but it's never been recognized. I might just say that the Institute for Disaster Research at Texas Tech has done considerable work on tornadoes. In fact, if given the opportunity to attend their symposium on tornadoes, which I think they have every two years, it's worth the adventure provided you can stand West Texas in the summer. They have a lot of meteorological engineering criteria for the tornado model that the NRC uses.

CHEEVER: Could strong ductwork downstream from HEPA filters protect the filters from tornado damage through frictional limitation of flow? Would this make it possible to omit the isolation valve?

PYSH: There are many things that can be done. I put them in a category of passive mechanics. If all you are concerned about is the ductwork, obviously it can be designed for three pounds and it will do the job. But there are filters and fans and other components.

15th DOE NUCLEAR AIR CLEANING CONFERENCE

CHEEVER: What I mean is, would you get enough losses in this ductwork by friction so you would protect the filters that way?

PYSH: I can't answer that question; it depends on the path and it has to be modeled. It's possible that it could be done.

ANDERSON: I might caution you about a navy test I observed one time. We had a guillotine, mushroom-type isolation valve to protect one of our buildings and we conducted a blast test against it. The guillotine worked fine, but the building disappeared.

15th DOE NUCLEAR AIR CLEANING CONFERENCE

EVALUATING NUCLEAR POWER PLANT VENTILATION SYSTEM ADEQUACY IN REDUCING AIRBORNE RADIOACTIVITY EXPOSURE

W. E. Jouris
King Faisal Specialist Hospital
and Research Centre
P.O. Box 3354
Riyadh, Saudi Arabia

Abstract

The problem of analyzing the effectiveness of the ventilation system for reducing airborne radioactivity exposure of personnel in a nuclear power plant is one faced by many nuclear analysis groups in power plant design organizations. This paper presents a rational way of approaching the problems and some simple methods of solving them. In so doing reasonable component leakage values are developed which can be used in solving this and other problems. For chronic leakage the values of 0.1lb/hr for valves, strainers and flanges are derived and 0.5lb/hr for pumps or other active components.

I. Introduction

Increasing attention is being given by the NRC (Nuclear Regulatory Commission) to in-plant radiological exposure and to keeping that exposure as low as reasonably achievable (ALARA) (1). One particular area of increased concern is the mitigation of airborne radioactivity. This is evidenced by the number of items concerned with this exposure source in NRC Regulatory Guide 8.8(1) and the questions concerning it in the latest revision of NRC Regulatory Guide 1.70.3(2). While it is evident that there is a connection between the ventilation in an area and the airborne concentration, it has not been clear exactly what the design relationship was other than increased airflow results in decreased airborne activity. Obviously, there are economic and practical constraints on this latter concept. The question to be answered then is what level of ventilation is necessary and practical and what are the factors affecting the selection?

II. Discussion

A primary source of airborne activity in an area in a nuclear power plant results from the leakage of contaminated liquids. This occurs through small leak paths such as valves, flanges, strainers, pumps and other such "breaks" in the piping and tankage systems. Open tanks or tanks vented into an area are even greater sources of airborne contamination than leaking components.

15th DOE NUCLEAR AIR CLEANING CONFERENCE

In general for an area:

$$\frac{dN}{dt} = - \lambda N + C_s F_i - F_o \frac{N}{V} + \dot{L} C_L P$$

where $\frac{dN}{dt}$ is the time rate of change of the airborne activity, λ is the decay constant for the radionuclide of interest, N is the total number of curies of the airborne radionuclide, C_s is the airborne concentration of the subject radionuclide in the incoming (staged) air, F_i is the incoming airflow rate, F_o is the outgoing air flow rate, V is the free volume of the room enclosure or other area of interest, \dot{L} is the radioactive liquid leak rate into the area, C_L is the subject radionuclide concentration in the leaking liquid and P is the partition factor of the subject radionuclide between the air and the liquid under the conditions extant. Under equilibrium conditions, this reduces to:

$$\frac{dN}{dt} = 0 = - \lambda N + C_s F_i - F_o \frac{N}{V} + \dot{L} C_L P \quad (1)$$

which is simply the familiar rate of input equals output plus accumulation with the added qualifier "minus decay." Re-arranging terms one can solve for the airborne concentration in the area:

$$C_A = \frac{L C_L P + C_s F_i}{(\lambda V + F_o)} \quad (2)$$

where C_A is the airborne concentration of the subject radionuclide equivalent to N/V for the simpler case of non-staged air flow (i.e., uncontaminated input air). For reasonable free volumes and moderate half lives, this equation reduces to:

$$C_A = \frac{L C_L P}{F_o} \quad (3)$$

While this equation is satisfied by any consistent set of units it is normal for the input data to be available with L in lbs/hr, C_L in uCi/ml, P is unitless and F_o in ft³/min. C_A is needed in uCi/cc to compare with MPC values. Hence a conversion constant of $5.34 \times 10^4 \frac{\text{ft}^3\text{-hr}}{\text{lb-min}}$ is necessary. Using the results of this equation,

one can now proceed to judge the adequacy of the ventilation as proposed for a building or alternatively to suggest a ventilation flow rate which will be adequate based on some pre-established criteria.

The decision as to what airborne concentration to allow in an area is a somewhat subjective one. From NRC regulations one might infer that as long as the total exposure does not exceed 40MPC hours per week to an individual the concentration in any area can be many times MPC. A more restrictive interpretation of 10CFR20⁽³⁾, however including the proposed 20.103 would lead one to the conclusion that airborne concentrations should be kept below 25% of MPC unless it is technically impractical to do so. Since it is necessary to post

15th DOE NUCLEAR AIR CLEANING CONFERENCE

an area as an airborne radioactivity area anyway if there is a reasonable chance that someone will be exposed to 25% of the limit, a prudent health physicist would no doubt post an area over 25% of MPC regardless of projected occupancy. Hence, to avoid unnecessary posting and to conform to the strictest interpretation of the code, a maximum of 25% of MPC is recommended as the design goal for airborne radioactivity in restricted areas. In conformance with our own practice with respect to skin dose rates and in the spirit of the ALARA philosophy, a design goal of 10% of MPC for airborne radioactivity in unrestricted areas is recommended. This latter would also make it permissible to tour minors into unrestricted areas of the plant.

III. Derivation of Leakage Terms

Liquid concentrations can be calculated with some measure of success and are necessary information for other radiological calculations during plant design. These parameters are usually known quantities. Likewise, the partition factor can be chosen from available data (such as in WASH-1248)⁽⁴⁾ knowing concentration and temperature of the liquid. One is left, therefore, with liquid leak rate and air flow rate as unknown variables. Since the appropriate air flow rate is the value sought, one is left with the problem of devising a method for arriving at the liquid leakage rate.

Some relevant value of leak rate must be assigned to each area of the plant. Should one pick a constant leakage, i.e., one gallon per minute and apply it to every area? Should the liquid leakage rate be based on the size of pipes that traverse an area? While many systems for assigning leakage or airborne concentrations to an area might be suggested, most of these "distribution formulas" would be open to serious criticism on one basis or another. The calculations would be simple and precise if daily leakage in each area of the plant is known. It is clear, however, that this leakage would vary widely with time and is not available at the design stage.

It was at this point that a more penetrating scrutiny of the sources of leakage in a plant was begun. Obviously, any "breaks" in the piping or tankage are potential sources of chronic leakage. It is the effects of chronic leakage which are to be mitigated. It is impractical to design ventilation to mitigate the consequences of a fountaining valve or a pipe break involving liquids of even moderate concentrations of iodine. The valves, flanges, strainers, pumps, etc., are easily identified as the potential and actual sources of leakage. They represent "breaks" in the otherwise continuous, integral path of piping and tankage. Attaching average leakage values to each component, however, proves to be a difficult and nebulous task. While a few values for such discrete leakage have been proffered in the literature, mainly traceable to B&W (Babcock and Wilcox)⁽⁵⁾ ⁽⁶⁾, no explanation is given for their genesis and, hence, it is impossible to attach a high level of confidence to the numbers. Such information (average leak rates per component) is typically not available given the host of variables involved such as valve types, sizes, materials, manufacturers, operating conditions and quality controls to name a few. It would be fortuitous if the

15th DOE NUCLEAR AIR CLEANING CONFERENCE

range of average leak rates taken over these variables proved to be confined to a narrow, useful band. It would be surprising if individual valves, throughout years of service and repair, remained in such a band. The possibility of finding component average leak rate data has therefore, been rejected and an entirely different tack taken.

To arrive at an appropriate rate for chronic leakage we must determine at what rate a component could leak undetected and unrepaired for the entire life of a nuclear power plant. When a component starts to leak, the liquid may collect on the bottom of the component and form drops which will drip. This phenomenon is essentially insensitive to the host of variables which characterize a valve as they influence only when the leak will start. Conceivably, every component in an area could leak at some low rate which would not be high enough to warrant repair or would escape detection. This is the maximum chronic leakage against which a ventilation system's radiological adequacy should be measured. While plant experienced persons will recognize that much higher leak rates occur routinely, these higher rates would not meet the criteria as chronic leaks, i.e., they would not go undetected very long, would be repaired at the earliest opportunity and would never occur on all components simultaneously without shutdown of part of the plant. Most importantly, leaks of this magnitude cannot be mitigated by practical ventilation design.

It remains to generate such values for chronic leakage. A simple experiment was performed in which the sweep second hand of a watch was observed while verbalizing the word "drip" at regular time intervals starting with one per second and working up to once every fifteen seconds. It seemed apparent that a drop every fifteen seconds would not be noticed by casual observation and that one every second would. Eventually, it was decided that one drop every five seconds might be noticed but would probably not be cause for repair action. Using a conversation factor of twenty drops per cubic centimeter, a chronic leak rate per component of 0.079 lb/hr was calculated. (This checks well, interestingly enough, with the B&W value of 0.0661 lb/hr which works out to 10 drops a minute or one drop every six seconds.) For computational ease as well as additional conservatism, this value was rounded to 0.1 lb/hr or approximately one drop every four seconds.

Pumps tend to leak more before being noticed and, in fact, are designed to leak some water for sealing, lubrication and seal cooling of shaft seals. Based on experience and some literature values ⁽⁵⁾ ⁽⁶⁾ it was felt five times as much leakage for pumps was appropriate. A value of 0.5 lb/hr as the chronic leakage of pumps for use in calculating necessary ventilation was, therefore, adopted.

IV. Application of the Technique

Having proposed the chronic leakage values, it remains to show how they are intended to be used. Rigorously, the adequacy of the ventilation in an area could be calculated by counting the exact number of leak paths in the area and multiplying them by the proposed

15th DOE NUCLEAR AIR CLEANING CONFERENCE

values to arrive at the total leakage. This, in fact, was done for one plant to test the technique. As might be expected, the method is extremely tedious, time consuming, and physically exhausting as it requires pouring over P&IDS (piping and instrumentation diagrams) trying to match up the components with the area under study. It requires that the design of the plant be advanced enough to have the P&IDS available. This sometimes means that it is too late to change ventilation design unless the change is critical as the equipment may have already been ordered. Through doing a plant the hard way, it was discovered that a certain maximum number of leak paths were infrequently exceeded. Adding a margin of safety, a value of 0.042 gallon per minute was determined as an upper limit on the chronic leak rate in any area. This value is used for screening in either of two ways: 1) when used with proposed ventilation flow rates to compare the resultant airborne concentration with 25% of MPC, or 2) to compare the calculated air flow rate with practical limits when an airborne concentration of 25% of MPC is used as the starting point of a calculation. Using this screening value, the separately ventilated areas of the plant can be expeditiously checked and the exceptions isolated. Generally, only a few areas will fail the screening tests. These few areas can now be checked with the more rigorous component counting technique to see if they really do not pass. Areas not passing the latter test require additional air flow or may require air flow at a level not practicable. In these cases, a decision must be made to either live with the potential problem with consequent administrative controls and posting or to take measures to affect one of the other variables in the equation.

It should be stressed that the minimization of airborne radioactivity by proper ventilation distribution should be considered as a fine adjustment on such activity. It is capable of minimizing the effects of only a narrow range of concentrations and, hence, liquid leak rates. The primary emphasis should be placed on eliminating leakage.

V. Other Factors to be Considered

While the primary emphasis of this article has been on the relationship of air flow rates to liquid leakage rates, a typical ventilation system review covers other less quantifiable areas. The ventilation system provides one of the prime agents in reducing the spread of airborne contamination. In this respect, a ventilation design should be checked to see that where air is staged (the air from one area also is used to ventilate another area) the flow pattern should be from areas of lower potential contamination to areas of higher potential contamination. The contamination potential of an area is based, of course, on the source strength in the area, i.e., radioactive concentration of the liquid (or gas). To prevent back flow from main ducts into areas or from a higher potential contamination area to a lower one, back flow dampers should be used on the exhaust duct from an area. Areas of potential contamination

15th DOE NUCLEAR AIR CLEANING CONFERENCE

should be maintained at lower pressures with respect to areas of no potential contamination. To maintain the latter, back flow dampers should also be installed on intake ducts into an area such that when a door is open into an area, the air flow is inward. Tanks should always be completely enclosed and the vents from tanks connected directly to the ventilation exhaust duct or as a minimum the vents should have local filters.

VI. Conclusion

No consideration has been given in this article to the industrial hygiene, thermal or comfort factors involved in ventilation design. While an impression may have been given that radiological considerations dominate the design of ventilation systems in a nuclear power plant, the reverse is almost always true. Generally, normal industrial requirements will provide more than enough ventilation to provide radiological adequacy as well. Frequently, the overabundant air flow in some areas based on industrial considerations will allow some re-routing of air flow to areas of radiological concern. It is rarely necessary for additional ventilation capacity to be installed for purely radiological considerations. A radiological review of ventilation design does insure that, given options, the designer will choose those with the least radiological problems. It also allows for the elimination of some potential problems prior to plant start up and the identification of some areas requiring initial attention.

VII. References

1. Information Relevant to Maintaining Occupational Radiation Exposure As Low As Reasonably Achievable (Nuclear Reactor), NRC RG-8.8 (Rev.1, September 1975) (U.S. Nuclear Regulatory Commission, Washington, D.C. 20545).
2. Standard Form and Content of Safety Analysis Reports of Nuclear Power Plants (Rev. 1, October 1972) NRC RG-1.70.3 (U.S. Nuclear Regulatory Commission, Washington, D.C. 20545).
3. Code of Federal Regulations, 10, Atomic Energy, Part 20, Standards for Protection Against Radiation (U.S. Government Printing Office; Washington, D.C. 1972).
4. Numerical Guides for Design Objectives and Limiting Conditions for Operation to Meet the Criterion "As Low As Practicable" for Radioactive Material in Light-Water-Cooled Nuclear Power Reactor Effluents, WASH-1258, July 1973. (U.S. Government Printing Office, Washington, D.C.).
5. WUPPS (Washington Utilities Public Power System) Preliminary Safety Analysis Report (U.S. Nuclear Regulatory Commission, Washington, D.C.).
6. Greenwood Nuclear Power Station Preliminary Safety Analysis Report (U.S. Nuclear Regulatory Commission, Washington, D.C.).

15th DOE NUCLEAR AIR CLEANING CONFERENCE

AIR CLEANING SYSTEMS ANALYSIS AND HEPA FILTER RESPONSE TO SIMULATED TORNADO LOADINGS

W. S. Gregory, R. W. Andrae, K. H. Duerre, H. L. Horak, P. R. Smith,*
C. I. Ricketts,* W. Gill*
Los Alamos Scientific Laboratory
Los Alamos, New Mexico
and
New Mexico State University
Las Cruces, New Mexico

ABSTRACT

A computer code, TVENT, for predicting tornado-induced depressurization in air cleaning systems is described. TVENT easily fits on many computers with input/output formats that are familiar to most analysts and HVAC designers. Our applications of TVENT to several nuclear facilities in Idaho, New York, and New Mexico are described.

Experimental results are described that provide supportive data on the response of individual air cleaning components to simulated tornado loadings. Peak pressure failure results for 610-by-610-mm-by-292-mm (24-by-24-in.-by-11-1/2-in.) standard HEPA filters have been obtained. Structural failure occurred for peak pressures of 9.7 kPa (1.4 psi) to 23.5 kPa (3.4 psi) at pressurization rates from 19.3 kPa/s (2.8 psi/s) to 9.7 kPa/s (1.4 psi/s), respectively. From these data, we derived a relationship between peak failure pressure and pressurization rate. Additional work is planned to evaluate the effects of manufacturer type, peak pressure duration time, number of filter folds, and filter orientation on structural failure.

Flow-resistance data of HEPA filters for use in TVENT are also described. At low flow resistance appears to be mainly caused by a diffusion mechanism, while at high flow the resistance seems to be caused by the mechanism of momentum exchange.

I. Introduction

Safety analysis reviews of proposed HVAC designs for nuclear facilities need to include the effects of tornados on air cleaning systems and the individual components within these systems. We have developed an analytical method to predict tornado-induced pressures and flows within nuclear facilities. This method has taken the form of an easily used, portable computer code called TVENT. We are also developing supportive experimental data of tornado effects on individual air cleaning components. Simulated tornado pulses are imposed on the components to determine their failure points and response at higher-than-normal pressures and flows.

*New Mexico State University, Las Cruces, New Mexico

15th DOE NUCLEAR AIR CLEANING CONFERENCE

A description of TVENT and examples of its application to nuclear facility air cleaning systems are described in the following sections. Also reported are experimental data on HEPA filter response to simulated tornado loadings. In addition, flow-resistance data on HEPA filters and integration of these data into TVENT are described.

II. Air Cleaning System Analysis

General

In setting out to develop TVENT, we assumed that to be analyzed, an air cleaning system had to exist either physically or as a finished design on architect-engineering drawings. We also assumed that, for maximum utility, the code must accept input in a form natural to designers of air cleaning systems.

With respect to the first assumption, we found that an air cleaning system does not have to exist physically or as a finished design before it can be analyzed. The computer code can be used in a design mode allowing the analyst to determine tornado transient effects at any time during the design phase. We believe that the code is also useful for determining the effects of minor perturbations (such as loss of a blower) in complex air cleaning systems. We believe our second assumption has produced a more useful code, as TVENT has been used by HVAC engineers that did not have extensive programming experience.

TVENT

TVENT solves steady-state and transient pressure distributions in complex ventilation networks and calculates system flow based on assumptions of

- o One-dimensional, isothermal flow,
- o Lumped parameters (neglecting spatial distribution of components), and
- o Incompressible flow with fluid storage at nodes.⁽¹⁾

Previous studies have shown that for tornado-induced flows inertial effects can be neglected and shock formation will not occur.^(2, 3)

TVENT is written in FORTRAN IV and is designed to be portable; that is, it can be easily transferred from one computer to another with a minimum of change. TVENT has been run on CDC, IBM, UNIVAC, and DEC computers, and requires less than 30K decimal words to run in a nonoverlaid mode on the CDC 7600 computer. The overlaid version of TVENT requires less than 20K decimal words on the same computer.

Input/Output

Input is organized and formatted in a way that is natural to the designer or engineer who prepares data for analysis. Input error

15th DOE NUCLEAR AIR CLEANING CONFERENCE

diagnostic messages are printed to help find errors in data preparation. Checks are made and messages are supplied when possible modeling errors are detected. Portability requirements precluded free format input and film plotting options, which are not found on some computer installations. Output lists and summaries are formatted and organized in a way that is helpful in determining the effects of a transient on system components and the integrity of pressure differentials between containment areas. Line printer plots for the time profiles of selected pressures and flows are also generated.

TVENT Application Examples

The degree of complexity needed in a TVENT model depends (1) on the purpose of the analysis, and (2) on the information available to define the system in its normal operating condition. It makes no sense to model a component that cannot be evaluated. On the other hand, those components (be they blowers, dampers, filters, or rooms) that significantly affect the system's performance must be represented. Certain portions of the model may be shown in much more detail than others depending on the desired refinement in output flows and pressures. Sometimes the effect of one part of the system on another can be crudely, yet accurately, simulated by the minimum number of components that are compatible with the pressure differentials in that area.

We have applied TVENT to a number of DOE nuclear air cleaning facilities to learn about the problems involved in such an application. In all but one case, the greatest difficulty encountered was with evaluating component performance during normal operation. Most of the information needed to define component effects (on the pressure) is not required for the operation of the system and, consequently, never measured in the field. The one exception, Los Alamos Scientific Laboratory's (LASL) new plutonium facility, involved a system that was not yet operational but could be completely defined by the architect-engineer's predictions.

The first application of TVENT was to the Idaho Chemical Processing Plant (ICPP) at Idaho Falls, Idaho.⁽⁴⁾ A recently installed atmospheric protection system (APS) was the subject of our analysis. This is an example of where the flows and pressures in a very specific part of the system are needed, but are not needed in the remaining parts. The TVENT model for this analysis is shown in Fig. 1. It shows the degree of modeling complexity judged to be appropriate for the older portions that are connected to the APS.

The second application of TVENT was to the new plutonium facility at the LASL.⁽⁵⁾ All of the information concerning the air cleaning systems was available from the architect-engineer's calculations and drawings. This proved to be a very worthwhile exercise in the development of TVENT because the application to such a large system tested TVENT's limitations. As a result, we know the code is capable of handling large systems. A small portion of the model used is shown in Fig. 2. This represents half of the first floor containing the laboratories and shops for the recycle and metal fabrication operations. The ducts terminating at the top of the figure lead to the basement that houses the 35 blowers servicing this area. The model of this system contained a total of 168 branches and 110 nodes.

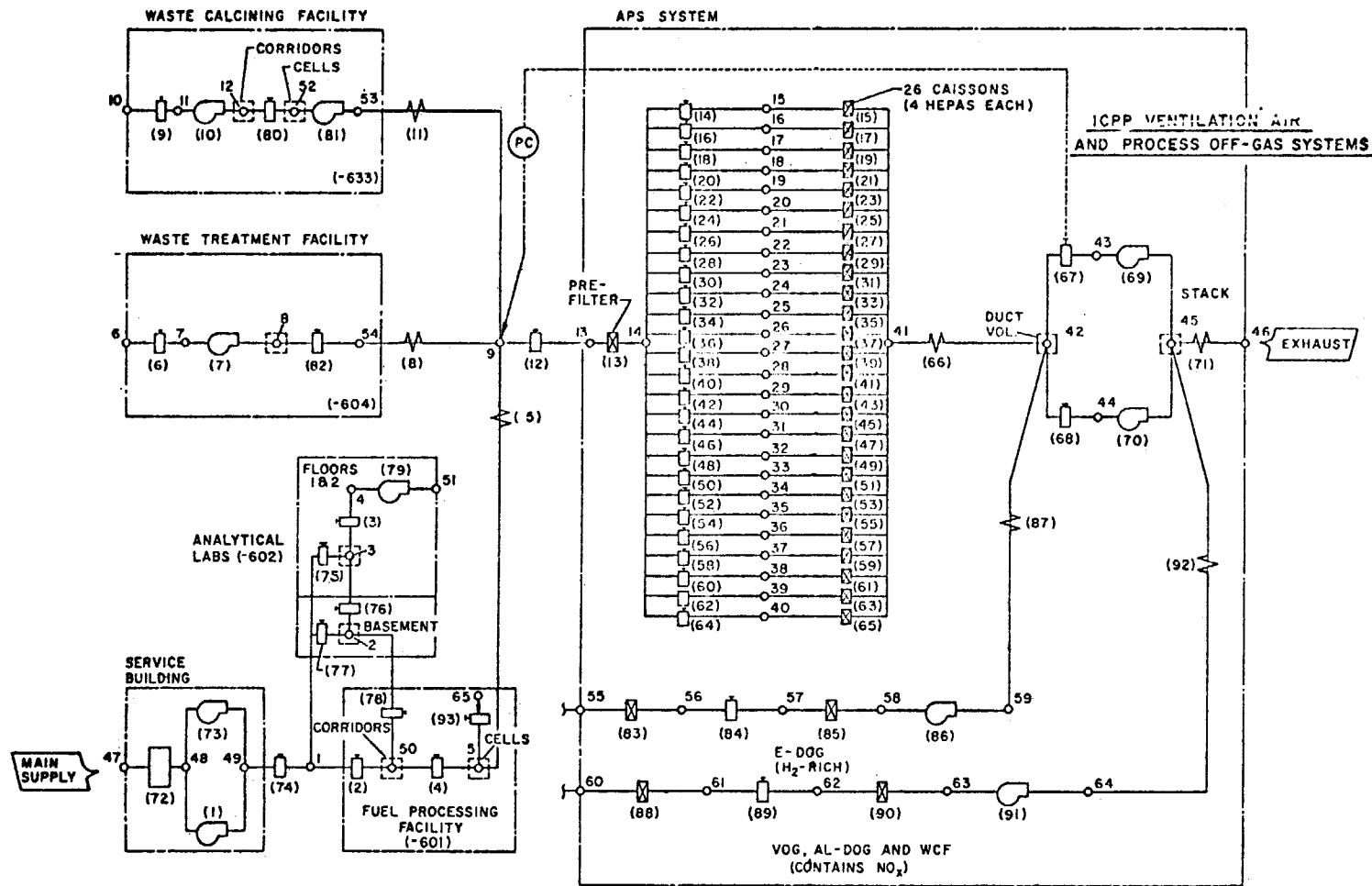


Figure 1 TVENT model of ICPP

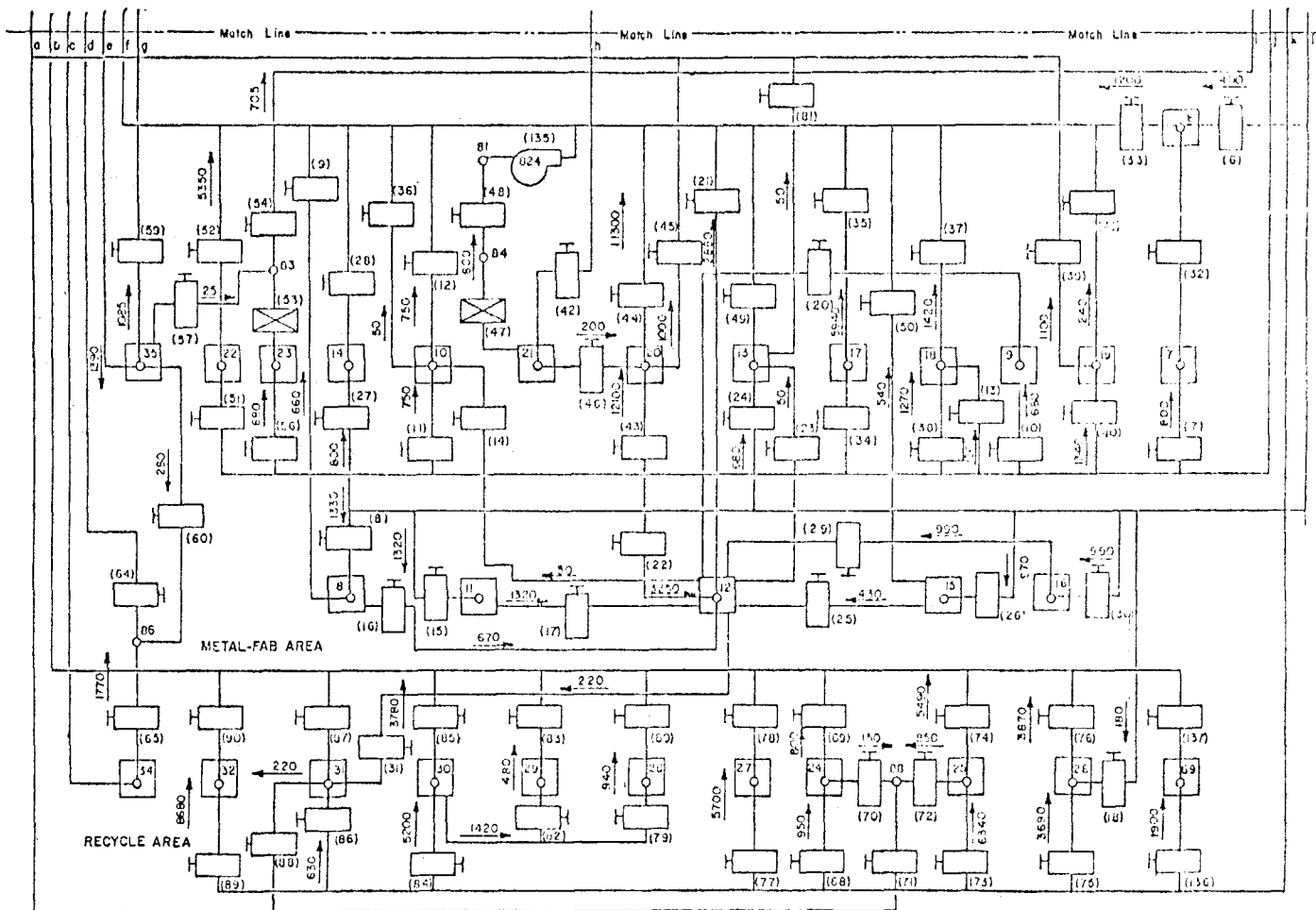


Figure 2 Complex TVENT model showing the LASL plutonium facility

15th DOE NUCLEAR AIR CLEANING CONFERENCE

The third TVENT application was to the head-end ventilation system at the Nuclear Fuel Services facility near West Valley, NY.⁽⁶⁾ The head-end system serviced the process building housing the major process cells used in reprocessing fuel elements. This facility is no longer operative, but residual contamination in these cells would present a potential danger if it were released to the surrounding environment during a tornado. The first step in studying this problem was to use TVENT to obtain the flows entering or leaving these cells during a hypothetical tornado. Figure 3 shows these flows as well as the flows in the ducts at the supply points for the tornado striking all supply points simultaneously. The duration of the applied tornado pulse was about 10 s and began at time = 10 s.

III. HEPA Filter Response to Simulated Tornado Loadings

General

Our studies of ventilation systems under tornado conditions also involve experimental work. We have fabricated a blowdown apparatus capable of generating transient air flow typical of a severe tornado through full-scale HVAC system components. The usefulness of this facility has been demonstrated by the testing of HEPA filters. We plan to use this facility in future tornado simulation experiments on other components as well.

The blowdown facility is located at New Mexico State University, Las Cruces, New Mexico. The test apparatus consists of an air compressor, two air storage tanks, sequencing valves, a prefilter chamber, and a test section. The sequencing valves control the airflow from the storage tanks through the prefilter chamber, test section, and finally, the test component. A high-speed movie camera was installed at the exit of the apparatus to study HEPA filter response to simulated tornado loadings. A more detailed description of the facility has been published.^(7, 8)

Initial Test Conditions

The purpose of our preliminary tests was to determine the relationship between failure pressure and the pressurization rate for standard 610-by 610-by 292-mm (24-by-24-by 11-1/2-in.) HEPA filters. Experimental determination of peak failure pressure required the sequencing valves to be set to give various pressurization rates. The rate specified in the National Regulatory Commission Guide 1.76 for a Design Basis Region I tornado (the most severe) is 13.8 kPa/s (2 psi/s). Filters were evaluated using pressurization rates at, above, and below this value. The tests were continued until the pressure differential across the filter was above the maximum of 20.7 kPa (3 psi) of the Region I tornado. The high-speed movie camera and all instrumentation recorders were started simultaneously with the sequencing valves. The actual times of filter failure were then found by observing the high-speed movies of the downstream filter face. Also photographed by the camera during the tests were a clock and manometer mounted beside the filters. Pressure differential across the filters and dynamic pressure were measured by electronic pressure transducers and recorded by strip chart recorders. Temperatures in the air storage tanks and the test duct were sensed by thermocouples and also recorded on the strip charts. Humidity was

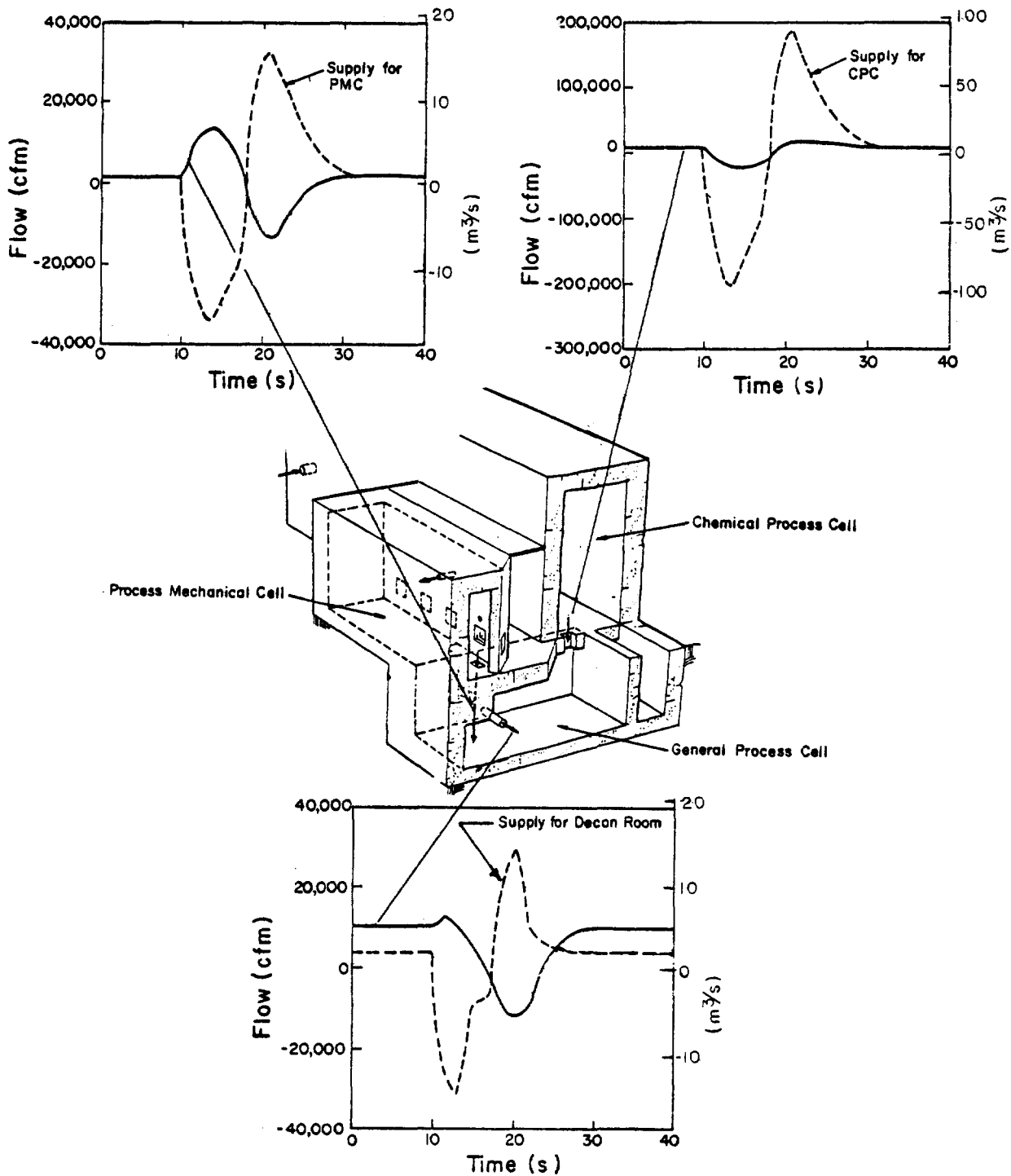


Figure 3 Nuclear Fuel Services cells and resulting transient flows

15th DOE NUCLEAR AIR CLEANING CONFERENCE

measured by a gauge within the prefilter chamber in the low velocity air. This gauge was read and the humidity recorded following each test.

Test Results

The test results are shown in Table I and Fig. 4.⁽⁹⁾ Eleven HEPA filters (from a single manufacturer) with 65 media folds were tested. The data of Table I indicate that structural failure occurred for a peak pressure range from 9.7 kPa (1.4 psi) to 23.5 kPa (3.5 psi) at pressurization rates from 19.3 kPa/s (2.8 psi/s) to 9.7 kPa/s (1.4 psi/s), respectively. Only two HEPA filters withstood the full 20.7 kPa (3 psi) transient pressure pulse. The column listed in Table I under "Break Fold No." indicates where the failure on the downstream filter face occurred. Medium folds were numbered left to right, 1 to 65. Thus in all but three cases, the glued, downstream edge of the filter medium was the initial point of weakness.

The data from Table I are shown plotted in Fig. 4. The solid line of Fig. 4 is a least squares fit to all the data. This fit indicates a trend in the relationship between failure pressure and pressurization rate. That is, the higher the pressurization rate the lower the pressure needed to fail the filters. Notice that the failure pressure at a pressurization rate of 13.8 kPa/s (2.0 psi/s) is

TABLE I. Experimental failure pressure vs. pressurization rate.*

Filter Serial Number	Pressurization Rate kPa (psi/s)	Failure Pressure kPa (psi)	Break Fold No.
41310250	9.0 (1.3)	21.4 (3.1)	1
41310358	9.7 (1.4)	23.5 (3.4)	65
41307976	9.7 (1.4)	13.8 (2.0)	1
41310360	10.4 (1.5)	15.2 (2.2)	65
41310366	11.7 (1.7)	17.9 (2.6)	38
41310859	13.1 (1.9)	17.3 (2.5)	35
41310283	13.1 (1.9)	15.2 (2.2)	65
41310363	13.8 (2.0)	14.5 (2.1)	1
41310268	18.6 (2.7)	16.6 (2.4)	65
41310367	18.6 (2.7)	20.7 (3.0)	28
41310261	19.3 (2.8)	9.7 (1.4)	1

*Note: All filters tested were 610-by 610-by-292 mm (24-by 24-by 11-1/2 in.) each having 65 folds.

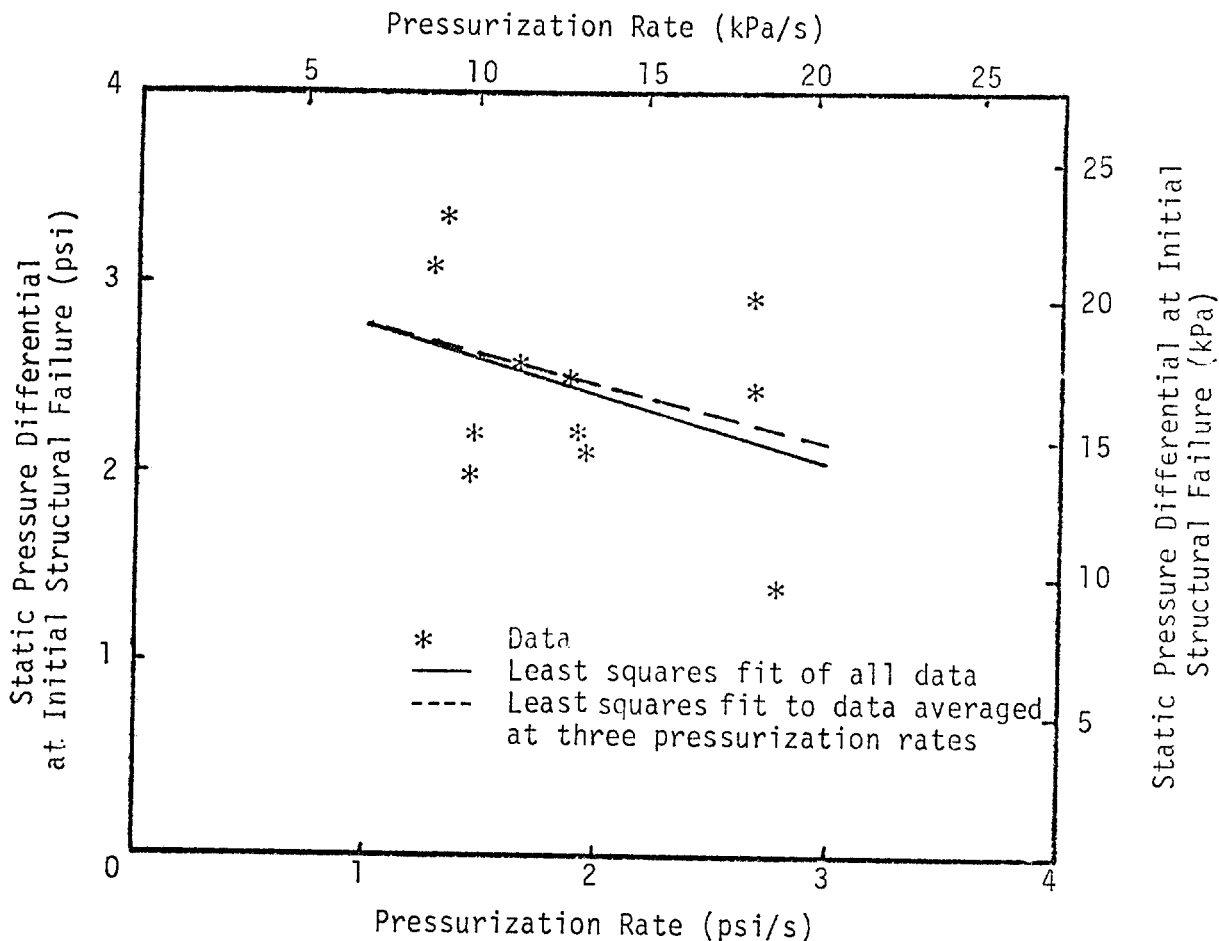


Figure 4 Static pressure differential at the point of initial structural failure as a function of pressurization rate [610- by 610- by 290-mm (24- by 24- by 11-1/2-in.) HEPA filters].

about 16.6 kPa (2.4 psi). Therefore, this type of filter would probably fail if subjected to a Region I tornado pulse. In fact, extrapolation of the least squares curve indicates that all filters of this type are in danger of failure at a 20.7 kPa (3.0 psi) differential pressure for pressurization rates above 3.5 kPa/s (0.5 psi/s).

The tests were run attempting to replicate failure pressure at three different pressurization rates. It proved difficult to repeat pressurization rates exactly. The three rates nominally were 9.7 kPa/s (1.4 psi/s), 13.8 kPa/s (2.0 psi/s) and 19.0 kPa/s (2.8 psi/s). If the data of Table I are treated as if the failure pressures indeed occurred at the nominal pressurization rates and are averaged for each rate, then the dotted line of Fig. 4 results. (The point with a pressurization rate of 11.7 kPa/s (1.7 psi/s) was not used in this analysis.) There is only a slight difference between this method of analyzing the data and taking a least squares fit of all the data.

The small number of filters available for testing did not permit us to obtain completely satisfactory results from a statistical

standpoint. Therefore, only very general conclusions can be drawn from the tests. First, there appears to be an inverse linear relationship between peak failure pressure and pressurization rate. Second, pressurization rates above 3.5 kPa/s (0.5 psi/s) seem too severe if these HEPA filters are to withstand a 20.7 kPa (3.0 psi) maximum pressure differential that would occur in a Region I tornado.

Flow-Resistance Data

The results of the resistance measurements on 610-by 610-mm (24-by-24-in.) filters appear to agree with earlier results obtained for 203-by 203-mm (8-by-8-in.) filters. These results are shown in Fig. 5. Diffusion and momentum exchange may be used to explain the shape of these resistance curves. At relatively low flow rates, the

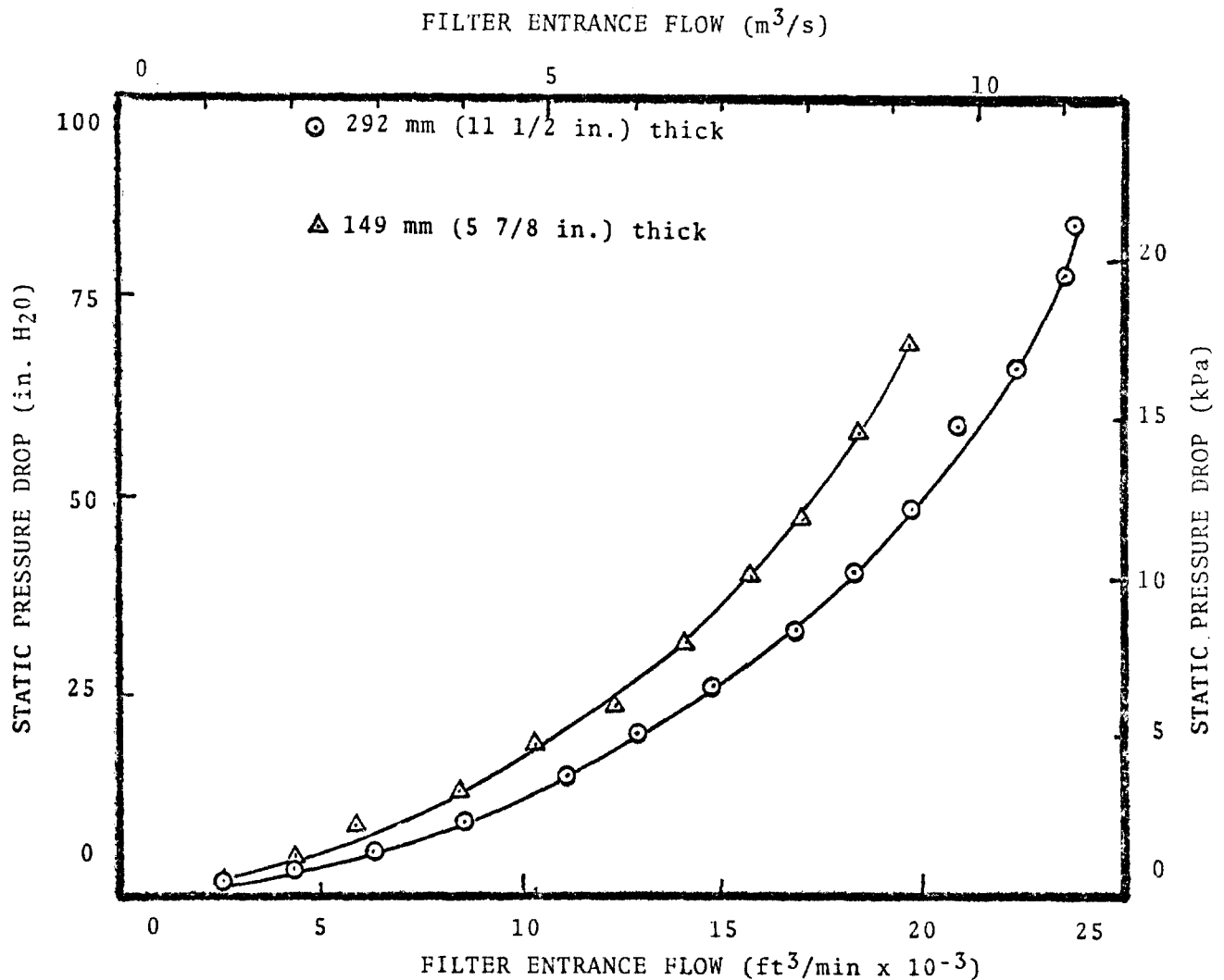


Figure 5 Resistance of 610- by 610-mm (24- by 24-in.) HEPA filters at high flow rates.

dominate mechanism causing resistance appears to be diffusion, while at higher flow rates, momentum exchange appears to dominate. When momentum exchange dominates, a majority of the flow is probably passing through the folded ends of the fiber mat only, thereby increasing the possibility of inefficient filtration.

IV. Future Work

- o Scale models of air cleaning systems have been constructed. We plan to obtain experimental data from these models and compare them with TVENT results.
- o Analytical development of an explosion computer code that is patterned after TVENT has been undertaken. This computer code will be capable of predicting internally generated pressure time profiles within air cleaning systems.
- o Structural tests will be performed on HEPA filters for simulated tornado transients to evaluate parameters of number of folds, time duration at peak pressure, manufacturers' types, and filter orientation.
- o Efficiency tests of HEPA filters under artificial loading conditions and airstream-entrained aerosol will be performed for simulated tornado transients. Particulate release vs dynamic pressure loading will be determined.
- o Shock tests of HEPA filters will be performed to evaluate both mechanical failure and particulate release. European, standard separatorless, flat pack, and American V-type will be evaluated.

V. Summary

In this report, we have described a computer code called TVENT that can be used by the designer and analyst to predict tornado-induced transients within air cleaning systems. TVENT is easily used, portable, and easily applied to diverse types of air cleaning systems. The computer code with its supporting documentation is available at the Argonne Code Center or through personal communication with the authors.

Structural response of HEPA filters to peak pressure differentials was described. Thus far, structural failure has occurred from 9.7 kPa (1.4 psi) to 23.5 kPa (3.4 psi) with one manufacturer's filters. There apparently is an inverse linear relationship between the peak failure pressure and pressurization rate. Nonlinear flow-resistance data at high flow rates were also obtained. These graphical data can be translated into empirical relationships and incorporated into the computer code TVENT.

Acknowledgements

The authors would like to express their appreciation for the support provided by the Department of Energy, Division of Operational and Environmental Safety, and Division of Waste Management. Support from the Nuclear Regulatory Commission, Division of Safeguards Fuel Cycle and Environmental Research is also greatly appreciated.

15th DOE NUCLEAR AIR CLEANING CONFERENCE

References

1. Duerre, K. H., Andrae, R. W., and Gregory, W. S., TVENT - A Computer Program for Analysis of Tornado-Induced Transients in Ventilation Systems, LA-7397-M, Los Alamos Scientific Laboratory, July 1978.
2. Bennett, G. A., Gregory, W. S., and Smith, P. R., Ventilation Systems Analysis During Tornado Conditions, January - June 1975, LA-6120-PR, Los Alamos Scientific Laboratory, Nov. 1975.
3. Gregory, W. S., Smith, P. R., and Duerre, K. H., "Effect of Tornadoes on Mechanical Systems," Proceedings of the Symposium on Tornadoes, Texas Tech University, Lubbock, Texas, June 1976.
4. Gregory, W. S., Andrae, R. W., Duerre, K. H., and Dove, R. C., Ventilation Systems Analysis During Tornado Conditions, October 1, 1976 - April 30, 1977, LA-6999-PR, Los Alamos Scientific Laboratory, Oct. 1977.
5. Andrae, R. W., Duerre, K. H., Dove, R. C., and Gregory, W. S., Ventilation Systems Analysis During Tornado Conditions, May 1, 1977 - September 30, 1977, Los Alamos Scientific Laboratory, report in printing.
6. Andrae, R. W., Martin, R. A., and Gregory, W. S., Analysis of Nuclear Facilities for Tornado-Induced Flow and Re-entrainment, Los Alamos Scientific Laboratory, report in printing.
7. Gregory, W. S., Horak, H. L., Smith, P. R., and Ricketts, C. I., Investigation of HEPA Filters Subjected to Tornado Pressure Pulses, LA-NUREG-6762-PR, Los Alamos Scientific Laboratory, 1977.
8. Gregory, W. S., Smith, P. R., Ricketts, C. I., and Reynolds, G., "Pressure Transients Across HEPA Filters," Seminar on High Efficiency Aerosol Filtration, Aix-en-Provence (France), November 1976.
9. Gregory, W. S., Horak, H. L., Smith, P. R., Ricketts, C. I., and Gill, W., Investigation of HEPA Filters Subjected to Tornado Pressure Pulses - Initial Structural Testing, LA-7202-MS, Los Alamos Scientific Laboratory, April 1978.

DISCUSSION

MURROW: Is this TVENT code available to anybody? Can we apply to you to run a simulation on a particular system?

GREGORY: Yes, the computer code is available to anyone who wants it. We have a manual that shows people how to use it and the code has been sent to the Argonne Code Center so all documentation and a listing of the computer code is available. We will be glad to help in any way that we can with regard to helping you with modeling. In the past, we have shown the architect engineers how to use it. Typically, it takes about half a day to just take one of their examples and go through it.

15th DOE NUCLEAR AIR CLEANING CONFERENCE

MURROW: Will this code take into account the resistances of the various components (e.g., filters and fans), flowrates, and volumes, etc.?

GREGORY: Yes, it will. There are high-flow-rate, pressure-type loading data that we still need in addition to HEPA filter data. One of the particular things we need relates to the fan response. We are trying to generate that type of data and we will put it into the code.

I must emphasize that much of the data in the experimental facility generates high flow rates. That's what you're going to get with a 3 PSI loading from the tornado. You're not going to get shock waves; it is not a shock loading facility. However, we are building a shock tube where we will be exposing some filters and other components to shock loads from internally generated explosions.

WARNKE: I would like to comment on your paper and the discussions related to tornado induced pressure transients in nuclear HVAC systems. With regard to Allied-General's spent fuel reprocessing plant at Barnwell, we ran an analog simulation of the HVAC system to verify the effects of tornado induced flow on HVAC systems in general and specifically on the final HEPA filter banks. The final HEPA filter bank for the process areas was sized for approximately 72,000 cfm (two 36,000 cfm banks). These were walk-in type filter plenums. The postulated tornado was taken as 0 to -3 PSI ΔP in 3 sec.; -3 PSI ΔP for 2 sec.; -3 PSI to zero PSI in 3 sec. Two cases were considered: (1) tornado at the supply unit, (2) tornado at the stack. The final exhaust filters were considered to have a loading of 5 in.w.g. at the time of a tornado. The tornado-induced flow raised the ΔP across the final HEPA bank to approximately 20 in.w.g. The blowers acted as a choke. With permission of my management I'll send you a copy of the Bechtel study.

CLOSING REMARKS OF SESSION CHAIRMAN:

The papers presented have informed us of the existence of a computer program (TVENT) for predicting steady state and tornado-(or extreme wind-) indicated transient flows and pressures in ventilation systems. For new facilities, many ventilation system alternatives can now be evaluated using the program, and an optimum design selected. The atmospheric parameters of a tornado have been identified and a facility constructed to duplicate these conditions in actual simulations. Preliminary experimental results have demonstrated both qualitative and quantitative tornado damage conditions for operational components.

An experimental facility was described that evaluates countermeasure devices and techniques for control of fires and/or fire related combustion products. Experimental data is now available for engineer/designers to optimize total system engineering parameters for fire protection.